Silicon Electrolyte Interface Stabilization (SEISta)

First Quarter Progress Report 2018

Anthony Burrell
National Renewable Energy Laboratory
15013 Denver West Parkway
Golden, CO 80401
Phone: (303) 384-6666
E-mail: anthony.burrell@nrel.gov

Brian Cunningham, DOE-EERE-VTO Program Manager
Hybrid Electric Systems, Battery R&D
Phone: (202) 586-8055
E-mail: brian.cunningham@ee.doe.gov

Table of Contents

Project Introduction

Silicon is a viable alternative to graphitic carbon as an electrode in lithium-ion cells and can theoretically store >3,500 mAh/g. However, lifetime problems have been observed that severely limit its use in practical systems. The major issues appear to involve the stability of the electrolyte and the uncertainty associated with the formation of a stable solid electrolyte interphase (SEI) at the electrode. Recently, calendar-life studies have indicated that the SEI may not be stable even under conditions where the cell is supposedly static. Clearly, a

more foundational understanding of the nature of the silicon electrolyte interface is required if we are to solve these complex stability issues. A new multi-lab consortium has been formed to address a critical barrier in implementing a new class of materials used in lithium-ion batteries that will allow for smaller, cheaper, and better performing batteries for electric-drive vehicles. This consortium, named the Silicon Electrolyte Interface Stabilization (SEISta) project, was formed to focus on overcoming the barrier to using such anode materials. Five national laboratories, are involved: NREL, ANL, LBNL, ORNL, and SNL.

The SEISta project was developed to specifically tackle the foundational understanding of the formation and evolution of the solid electrolyte interphase on silicon. This project will have as its primary goal an understanding of the reactivity of the silicon and lithiated silicon interface with the electrolyte in lithium-ion systems. It consists of researchers from multiple national laboratories (ANL, SNL, ORNL, LBNL, and NREL) working toward clear unified goals. The Silicon Deep Dive team which is focused upon the science and technology barriers in functional electrodes is a critical partner in this work. Many of the researchers are shared between both teams and we hold joint meetings to ensure effective communication between the teams.

The current goals of SEISta are:

Quarter 1 Milestone:

Have completed the selection and characterization (XPS, SIMS, IR, and Raman), including determination of the surface termination chemistry and impurity levels, of the SEISta model research samples to be used by all members of the team in FY18.

Quarter 2 Milestone:

Have characterized (XPS, SIMS, IR, and Raman) the surface chemistry and composition of the SEISta model research samples after contact with the electrolyte, before cycling, including the nature of the electrolyte decomposition products.

Quarter 3 Milestone:

Completed characterization (electrochemistry, IR and Raman) of the early stage silicon electrolyte interphase formation on the SEISta model research samples, specifically by establishing and demonstrating a procedure for quantitatively measuring the solubility of SEI on silicon surfaces.

Quarter 4 Milestones:

Established and demonstrated a procedure for measuring the growth rate of silicon SEI components at fixed potentials and during cycling.

Have determined how the physical properties of the silicon electrolyte interface are influenced by the nature of the silicon surface on the SEISta model samples.

Approach

The SEISta team works to ensure that protocols for sample preparation, experimental design and implementation, as well as data reporting are consistent across the whole team. Each laboratory is working toward the same set of quarterly milestones using its own specific talents and capabilities in a concerted effort with the other team members. This joint focus results in multiple researchers interacting to produce and analyze data to ensure that individual experimental variations will not lead to erroneous results. Critical to the success of this effort is the use of standard samples that can be shared by all parties. In the first FY, a round-robin sample test was established to ensure that data could be duplicated at the different laboratories by different researchers. In addition to weekly whole-team video presentations, we have held on-site face-to-face

meetings each quarter for all team members, and other interested parties, to brainstorm and sort out issues with existing experiments and jointly develop new experimental plans.

The outcomes from FY17 indicated that the nature of the silicon starting materials has major implications for the formation and evolution of the SEI. This is most clearly seen in the inherent chemical reactivity of the silicon materials with electrolytes before electrochemistry. Much of our focus for FY18 will be in looking at the initial chemistry of the silicon on contact with electrolytes. This will then lead to an understanding of how the electrode electrolyte interface changes upon applied voltage and how the SEI forms and eveolves.

Objectives

The critical issues SEISta is attempting to determine are:

- What are the properties of the lithiated silicon electrolyte interface?
- What is the Silicon SEI actually made of and what reactions are contributing to it?
- How fast does the Silicon SEI grow?
- Does it stop growing?
- Is it soluble?
- Can it be stabilized?

For this quarter the team focused on three broad tasks:

Materials Standardization – This task is critical to the development and deployment of standardized samples and experimental procedures across the team. We will continue to provide full characterization to any new sample that is to be used for SEI studies to ensure reproducibility and full understanding of the material. This Quarters work on the reproducibility of sputtered samples and their electrochemical performance across the laboratory partners was a significant continuation of this effort. The nature of the dry box environments for assembling and testing appears to be a factor in the reproducibility of the samples. Also the aging of these samples has a marked effect on the consistency of the data. We also focused upon the preparation of new wafer samples with controlled oxide coatings. The development of a procedure to dial in the thickness of the oxide coating in standardized samples is critical for moving into the next quarters. In addition, cell design and electrochemical standardization of the wafer samples begun in this quarter will continue as we move forward.

Model Materials Development and Characterization – The nature of the electrode-electrolyte interaction in silicon electrodes is at the heart of the formation and stability of the SEI. The inherent chemical reactivity of silicon with common electrolytes has been a focus for this team and will be a primary focus moving to quarter 2. The synthesis of well-defined silicon nanoparticles and the different chemical markups of lithiated silicon surfaces is being probed by preparing model compounds and thin films that may/can exist in silicon anodes. Lithium silicides, silicates, and other inorganic material (LiF, Li_2O) are being prepared and their reactivity with electrolytes is being determined. These materials also act as standard spectroscopy samples for the researchers who are looking at the formation of the SEI on different silicon materials.

SEI Characterization – The overall objective for SEISta is to understand the nature and evolution of the SEI on silicon anodes. The materials standardization and model compounds will enable the researchers to systematically investigate the formation of the solid electrode interphase using a wide variety of the spectroscopy techniques, from different optical, microscopy, and electrochemistry to determine how the SEI forms based upon the nature of the silicon surface, and how it evolves over time.

Milestone Quarter 1 FY18 - Silicon Electrolyte Interface Stabilization (SEISta)

SEISta Team

Background

The overall objective of the SEISta project is to better understand the formation and evolution of the solid electrolyte interphase (SEI) on silicon anodes. Silicon is a viable alternative to graphitic carbon as an electrode in lithium-ion cells and can theoretically store >3,500 mAh/g. However, lifetime problems have been observed that severely limit its use in practical systems. The major issues appear to involve the stability of the electrolyte and the uncertainty associated with the formation of a stable solid electrolyte interphase (SEI) at the electrode. Recently, calendar-life studies have indicated that the SEI may not be stable even under conditions where the cell is supposedly static. Clearly, a more foundational understanding of the nature of the silicon electrolyte interface is required if we are to solve these complex stability issues. A new multi-lab consortium has been formed to address a critical barrier in implementing a new class of materials used in lithium-ion batteries that will allow for smaller, cheaper, and better performing batteries for electric-drive vehicles. This consortium, nicknamed the Silicon Electrolyte Interface Stabilization (SEISta) project, was formed to focus on overcoming the barrier to using such anode materials. Five national laboratories, led by the National Renewable Energy Laboratory (NREL), are involved: NREL, as well as Argonne (ANL), Lawrence Berkeley (LBNL), Oak Ridge (ORNL), and Sandia National Laboratories (SNL). The first quarter milestone for SEISta in FY18 was:
To have completed the selection and characterization (XPS, SIMS, IR, and Raman), including determination of the surface termination chemistry and impurity levels, of the SEISta model research samples to be used by all members of the team in FY18.

Results

This objective was 100% completed.
Several different research samples are used as standard materials in the SEISta project. Thin-film sputtered silicon samples provide amorphous silicon electrodes. In addition, doped silicon wafers with controlled oxide coatings are employed. We have multiple sources of each type of samples and these are utilized by the research team to look at different aspects of the SEI formation and evolution. The 1st quarter milestone was to enable the whole team to have confidence that the research materials were consistent from lab to lab.
The thin film samples characterized in quarter 1 came from both ORNL and SNL. The first set of films consisted of amorphous silicon deposited on battery-grade copper foil (ORNL). The films were deposited at an applied power of 90 W at a distance of 7.0 cm from substrate to target. Samples were deposited at 7.0 mtorr of argon pressure, which is the same pressure used to deposit the sample used for the Neutron Relectrmetry (NR) studies. The thickness of the films was determined to be 55 ± 2 nm based on quartz-crystal microbalance and neutron reflectometry measurements. The density of the films was estimated to be 2.1 g/cc from the NR data. (reported in FY17 annual report)
A second set of films were prepared, at SNL, in a similar fashion with the difference being the sample substrate was a copper coated silicon wafer. These new thin film samples shown in figure 1 have the advantage of an inflexible current collector but are not designed for coin cell and related electrochemical cells.

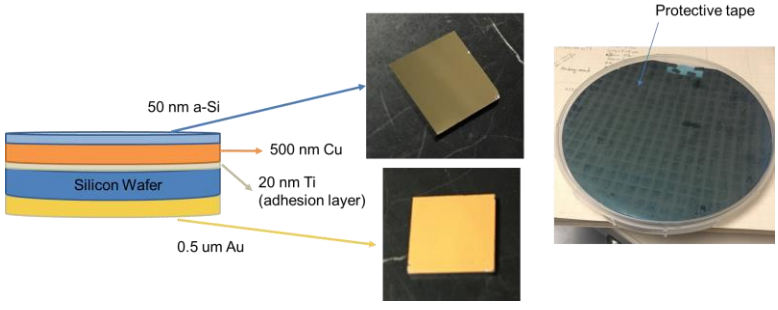

Figure 1 Thin film wafer samples prepared on silicon wafers.

Significant analysis of the new wafers was carried out (XPS, SIMS, IR, and Raman, as required by the Q1 milestone) to identify the surface and how that surface is affected by the silicon masking used to produce the wafers and an example of the IR spectroscopy is shown in Figure 2.

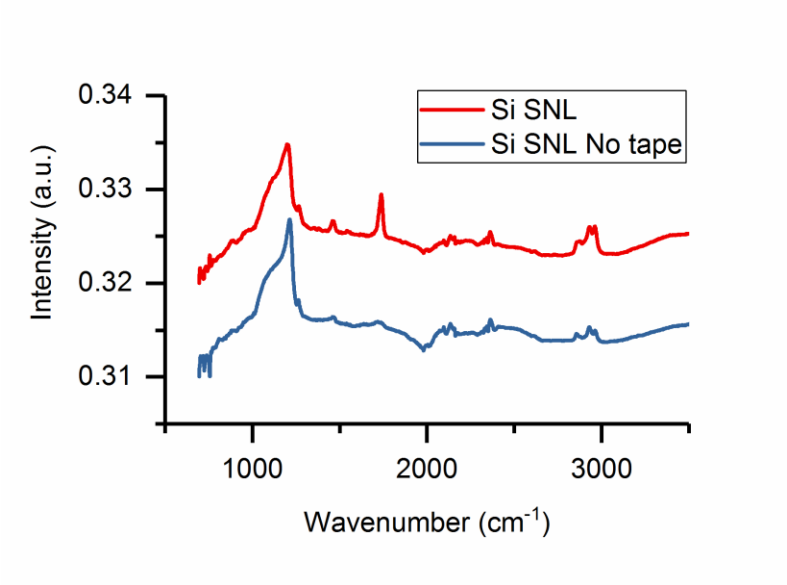

Figure 2 example of the IR spectra of samples prepared with and without tape. C-O and C-H vibrations were observed in both samples, but are more pronounced in the tape samples.

The amorphous silicon samples were extensively characterized using XPS, SIMS, IR, and Raman and electrochemical performance. The variability between research groups and the potential for local contamination was tested using a set of samples prepared at ORNL, shipped to all labs for testing, followed by extensive comparison of the samples (pre-and posttest) at NREL. The details of these experiments are described within the accompanying Q1 quarterly reports.

For wafer samples the nature and selection of the oxide coating and how effective back electrical contacts are made was investigated. Oxide coated wafers were purchased commercially, and the oxide coating was analyzed and the data is reported in the accompanying Q1 quarterly reports. Additional aspects of this work were the control of the oxide thickness and the effective formation of the back contact.

Conclusions

The milestone was 100% completed, and research samples were characterized for the SEISta team. However, the nature of the dry-box environment at different laboratories is a factor in the initial cycling for the thin film samples on copper foil. As the SEI formation in the first cyclic is expected to be critical to the development and evolution of the SEI on silicon this potential variable will need to be considered in future experiments.

Materials Standardization - Electrode Aging (ORNL)

Gabriel M. Veith (ORNL), Kevin Wood (NREL), Steven Harvey (NREL), Christopher Apblett (SNL), Chunmei Ban (NREL), Atetegeb Haregewoin (LBNL), Binghong Han (ANL), Jack Vaughey (ANL)

Background

The program performed an initial round robin experiment to evaluate the cycleability and reproducibility of electrodes prepared by vapor deposition. The initial results were unimpressive and broad. Thorough analysis of the data revealed significant differences in aging times and conditions between the partner laboratories. In an effort to elucidate the magnitude of these effects and identify the potential limits of vapor deposited silicon electrodes a smaller, more focused, and highly regimented study was organized and performed. In addition to

the cycling experiments studies were performed to evaluate glove box impurities. This work is important towards the "determination of the surface termination chemistry and impurity levels, of the SEISta model research samples to be used by all members of the team in FY18."

Results

For these experiments two sets of 50 nm Si films were deposited on battery grade copper foil. 12 mm electrodes were punched out and packaged for shipment to the partner laboratories. In addition to the electrodes complete coin cell kits, separators, pipets, and cycling protocols were sent to each of the partner laboratories along with detailed preparation procedures, and timelines. Each partner lab was required to purchase the correct Li foil, Eppendorf type pipet, Li cleaning and polishing supplies. The benefit of this level of detail was the elimination of impurities, differences in hardware, aging, and areas. In addition, each team was sent high surface area TiO_2 and extra Si films to probe the chemistry of their glove boxes. These samples were aged in place for 5 days and shipped to NREL for analysis.

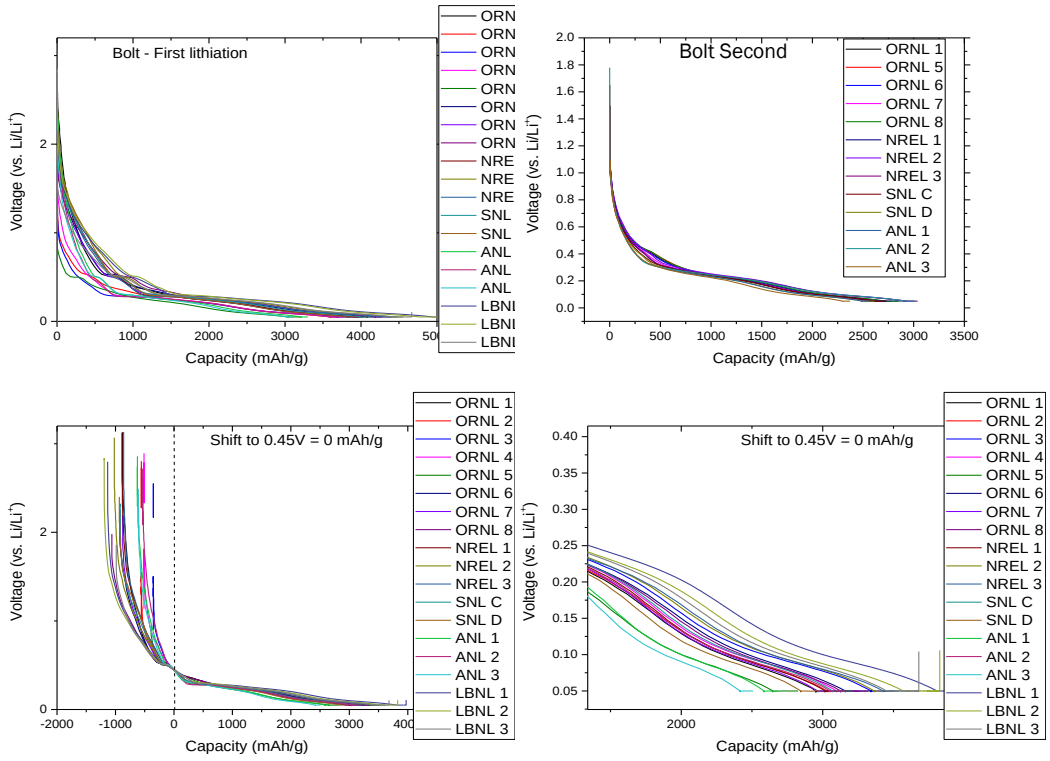

Figure 1. Top Left – Raw lithiation data measured for the first cycle; Top right – Raw lithiation data for the second cycle; Bottom left, first lithiation data shifted to 0.45V; Bottom right – Zoomed in view of shifted data.

Figure 1, top left, shows the cycling data collected at each laboratory for two batches of materials. The cycling followed a constant current/constant voltage protocol (C/10 to 0.05V). There appears to be a large variation in capacity upon the first lithiation (~1000 mAh/g). The data for all the samples has a clear plateau around 0.55 V (vs. Li/Li^+) which is attributed to SEI formation since this is above the insertion potential of Li within Si. When the data is normalized to 0.45 V (vs. Li/Li^+) the capacity of the films becomes very reproducible (~3400 mAh/g), after the constant voltage step, and is consistent with the predicted capacity of Si anodes (~3600 mAh/g), Figure 1 bottom right.

The difference in capacity (~700 mAh/g) is attributed to reactions that occur at potentials greater than 0.7 V (vs. Li/Li^+). These reactions point to impurities in the electrolytes or impurities in the electrodes. Interestingly, this high voltage capacity is about 50-100% smaller than the same capacity observed in the original round robin experiment (FY 17). This means that sample aging is critical to reproducibility AND/OR the choice of coin cells, the drying of materials, or the volume of separator has a significant influence on reproducibility.

The control samples of TiO_2 and sputter deposited Si films showed large variations in surface chemistry after exposure to the glove box atmospheres at the respective partner labs. Indeed, XPS and TOF-SIMS data collected at NREL showed variations in carbon, oxide and fluoride impurities originating from the glove box, Figure 2. It is not clear if these variations cause the observed changes in capacity of if the electrolyte is an issue.

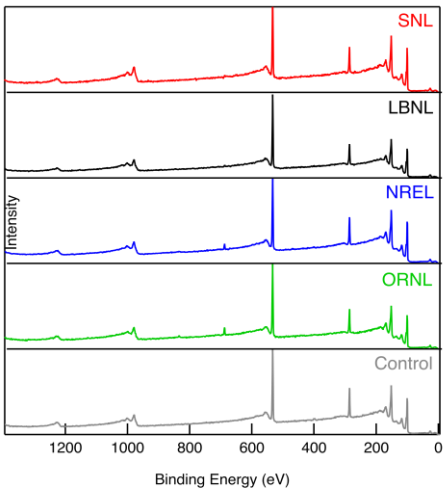

Figure 2. XPS spectra collected on witness Si electrodes

Interestingly, upon the second lithiation the variation in capacity for the films is virtually eliminated, Figure 1 (top right). This is a significant improvement over the first cycle and an improvement over the original round robin data. This further indicates that a surface impurity or electrolyte impurity is reacted away during the first lithiation process.

Conclusions

This data indicates that an impurity dominates the initial cycling capacity. Future studies with $LiFePO_4$ electrodes are planned to determine if this impurity originates from the Li or differences in the Li surface after cleaning. In addition, it still needs to be determined which batch of samples some of the electrodes in this study came from to isolate the problem further.

Materials Standardization- Preparation of Oxidized Silicon Wafer Surfaces for Electrochemical Testing (NREL)

Manuel Schnabel (NREL), Matt Page (NREL), Paul Stradins (NREL)

Background

Polished silicon wafers provide the most controlled silicon material with which to study the fundamental processes occurring during the lithiation of silicon from an electrolyte. We have previously reported on a cleaning routine adapted from the electronics industry that was applied to hundreds of samples for round robin measurements within this project. This quarter, we have looked into preparing oxidized silicon surfaces with precisely controlled SiO_2 thicknesses, and improving the rear side contact to the silicon.

Results

1. **Oxidizing silicon wafers to different, but comparable oxide thicknesses** is difficult due to strong and non-linear time and temperature dependences. However, thick (>100nm) oxides can be wet-chemically thinned in a precise way, which was the goal of our research this quarter.

In silicon processing for electronics, a buffered oxide etch is typically used when control of the etch rate is required, which consists of a 1:6 or 1:7 mix of bottle-strength HF and NH_4F. HF is a weak acid, so the solution pH can be buffered by a conjugate base such as NH_4F. However, the industry-standard solution

etches too fast for nm-level control over the final thickness. We therefore started from this concentration ratio and prepared a solution of 1M HF and 7M NH_4F in DI water, then diluted the solution to an etch rate of ~20nm/min. The resulting solution has a predicted pH of 3.50 and measured pH of ~3.4, which is close enough to the pKa=3.15 of HF to act as a pH buffer. Figure 1 shows the results from 4 samples thinned simultaneously in a flower holder - thicknesses are measured between etch steps using spectral ellipsometry. The mean square error of fitting a flat SiO_2 film to the data does not increase as etching progresses, indicating that the film does not roughen appreciably (it also retains a polished appearance).

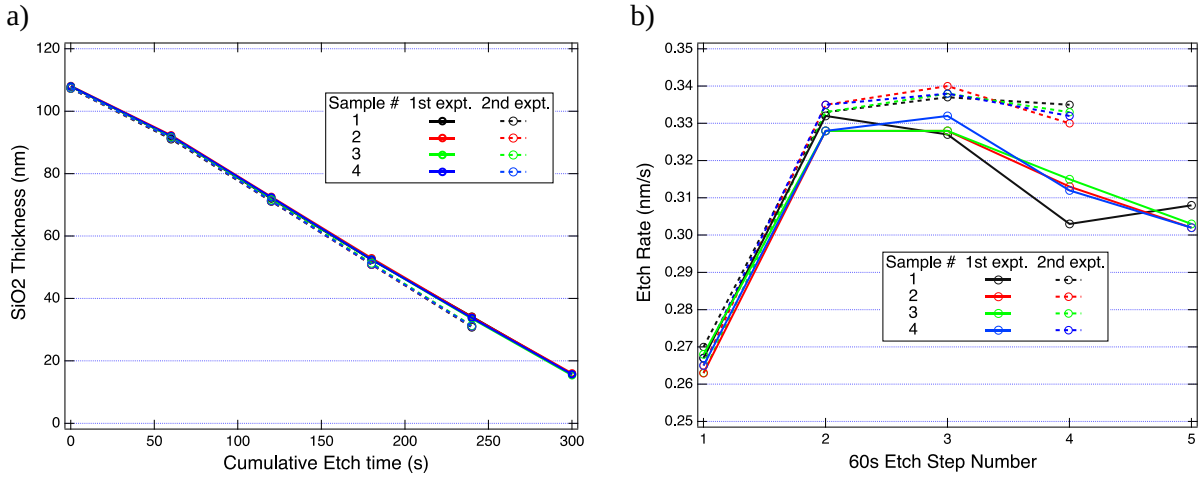

Figure 1: SiO_2 thinning results in dilute HF:NH_4F solution. Two experiments a few days apart are shown. (a) SiO_2 thickness remaining as a function of cumulative etch time. (b) Etch rate during each etch step. It can be seen that thinning is very homogeneous across samples, and rates are quite stable after the first etch step.

In each of the two experiments depicted in Fig. 1, 70-100nm SiO_2 are removed by the end, and the thickness removed differs by no more than 0.5nm across the 4 samples processed simultaneously in a flower holder. Furthermore, neglecting the first etch step (which differs because the first few nm at the sample surface etch slower) the etch rate is quite consistent, ranging from 0.30-0.34nm/s (provided the solution temperature is 23°C). This is sufficiently slow that human error in timing the etch can be expected to result in errors <1nm. We are therefore confident that we can fabricate large batches of samples with oxide thicknesses in the range of 10-100nm, and differing less than ~3nm across a batch.

2. When using silicon wafers as anodes in electrochemical cells, it is also important to form a **good electrical contact** to the back of the wafer to keep the voltage dropped across that contact as low as possible. Assuming current densities of up to 10mA/cm^2 and an anode area of 1cm^2, up to 10mA must be passed through the contact to the wafer. As can be seen from Figure 2, this is non-trivial for silicon if the doping density is insufficient for the silicon to be quasi-metallic, resulting in a potential drop of ~500mV across a ~0.1cm^2 silver paint (Leitsilber) contact. Metallic indium solder, and InGa eutectic liquid metal, are found to perform much better, yielding ~100mV potential drops for ~0.05cm^2 contacts. This represents a contact resistivity of 5Ωcm^2 for silver paint, and 0.5Ωcm^2 for indium solder or InGa eutectic.

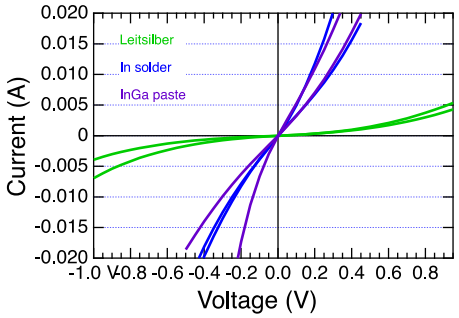

Figure 2: Current-voltage curves measured across pairs of contacts made to deoxidized and scratched Si wafer surfaces (wafer doping is ~4x10^{18} cm^{-3}, which can make contacting difficult). It can be seen that the ~0.1cm^2 silver paint (Leitsilber) contacts are rather mediocre, whereas 0.05cm^2 In solder or InGa paste contacts perform much better.

Even 100mV voltage drop over a contact is too high for precise electrochemical measurements; however, the value can be reduced by increasing the contact area. Generally, contact resistance is inversely proportional to the area (it is given by the aforementioned contact resistivity divided by area), so increasing the In solder or InGa paste contact area from ~0.05cm^2 to the full 1cm^2 electrode area lowers the resistance 20-fold to 0.5Ω, and thus the potential drop associated with 10mA to only 5mV. These considerations and preliminary results (above) highlight the need to precisely define the contact resistivity that results in low contact resistance. For example, a simple mechanical contact (e.g. by metallic screw) might provide good contact resistivity, but because of a very small contact area, the resistance could still be high. Conversely, a metal paint contact might be beneficial if spread over a whole area despite its relatively high contact resistivity. Further improvements are possible if the area of the rear contact is made larger than the active anode area within the cell, which could be realized by masking much of the cell-facing side of the silicon wafer with an insulator that is impermeable to Li. Lastly, the potential drop scales linearly with current for an Ohmic contact, so performing experiments at <0.1mA/cm^2 largely avoids these issues. Nevertheless, we will also pursue improvements in contact materials in the next quarter in order to develop a simpler method for achieving negligible voltage drop across the silicon wafer contact.

Conclusions

A method to thin SiO_2 layers at ~20nm/min with sub-nm variation in thickness across simultaneously processed samples was developed, and will be deployed in half-cells in the next quarter. Initial progress has been made on good contacts to Si wafer anodes, but more work is required in the coming quarter.

Materials Standardization – Electrochemical Behaviour of Silicon Wafers (NREL)

Lei Cao, Yanli Yin, Taeho Yoon, Chunmei Ban (PI), NREL, Golden, CO

Background

The objective of this project is to develop a fundamental understanding of solid electrolyte interphases (SEI) for silicon (Si)-based electrode materials, and provide practical strategies for stabilization of the SEI in Si-based electrodes. The SEI layer begins to form as soon as the Si electrode contacts the electrolyte. The SEI is comprised of the products from many reduction reactions of salts, solvents and impurities. These reduction reaction competes with each other; and the kinetics is heavily dependent on current density, overpotential and the catalytic properties of the electrode surface, finally determine the composition of a SEI. Regarding the silicon anode, the volume changes caused by the lithiation/delithiation process present new challenges. The continuous reduction of electrolyte may be attributed to the unceasing appearance of new surface during the volume changes, which can obsfuscate the study of the interaction between the electrolyte and the Si surface. In order to decouple

the interfacial chemistry from the interference of the volume changes, here, we aim to investigate the early-stage SEI chemistry before the Si lithiation process. This approach enables the study of the sole impact of early-stage SEI on the composition of SEI and the electrochemical behaviors. Furthermore, the information collected from the early-stage SEI could provide the new strategies to stabilize the Si electrode surface.

The intrinsically high sensitivity of SEI to the reaction environment and the surface structure and morphology has contributed to the measurement discrepancies, which causes significant difficulty in fully understanding the chemistry of SEI. Therefore, we have firstly established standard model Si electrodes, cleaning protocols, and cell fabrication procedures to elucidate the convoluted mechanisms of SEI on Si-based electrodes.
Milestones

- Define the formation of the early-stage SEI for the Si model electrode. (Jan 15th 2018)
- Demonstrate the effect of the electrolyte composition ($LiPF_6$ and LiTFSI based electrolytes) on the formation of the early-stage SEI . (Mar 30th 2018)
- Modify the surface of the Si model electrode with lithium carbonate (nonconductive) and carbon (conductive) coating and evaluate the coating impact on the formation of the early-state SEI. (Jun 30th 2018)
- Summarize the effects of the electrolyte composition and coating materials on the chemistry of the early-stage SEI. (Sept. 30th 2018)

Results

Cell fabrication. Silicon model samples established in FY17 have been used in this study. All of the Si electrodes (½ inch x ½ inch) were cleaned with our established multi-step cleaning protocol to remove the surface grease, particles and organic residue. After cleaning, the electrodes were dried in vacuum oven at 100 °C prior to the cell fabrication. **Electrochemical properties.** Due to the low electrical conductivity and the brittleness of Si wafer electrode, the pressure on the electrode plays an important role in the electrochemical behavior of the cell. As shown in Fig. 1a, reversible electrochemical cycling data can be only achieved when using appropriate pressure on the Si electrodes.

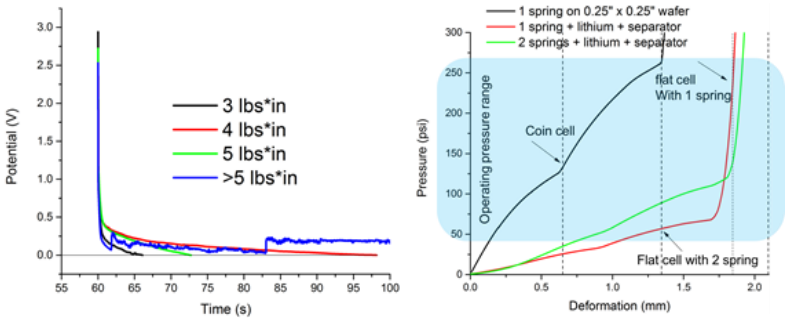

Figure 1. (a) Electrochemical voltage profile of Si wafer electrode at various pressure; (b) The plot of the pressure on the electrode as a function of thickness change (deformation, measured before and after the cell crimping) in the cell.

Higher pressure may accelerate crack initiation and propagation, while the low pressure failed to enable good electronic contact between the Si wafer and the current collector. Fig. 1b displays the comparison of the pressure in different assemble conditions. In our case, the wave spring has been used to adjust the pressure in different cells including the coin cell and the flat cell developed in the group. All of electrochemical data were collected in the flat cells under operating pressure range. **Define the early-stage SEI.** Galvanostatic lithiation/delithiation was performed on the Si model electrodes with various current density, as shown Fig. 2a. Differential capacity analysis (dQ/dV) was used to monitor the reduction of electrolyte and the Si-lithiation process, as plotted in Fig. 2b. The reduction of the electrolyte starts much earlier when using lower current, as compared to those with higher current. The electrochemical activities above the Si lithiation process contribute to the formation of early-stage SEI. The research focuses on the investigation of the electrochemistry related to the formation of early-stage SEI. It shows that the side reactions during the early-stage SEI formation has been suppressed when using

large current. One hypothesis for the mitigated reduction reactions is that the increased overpotential of the side reactions affects the chemistry of early-state SEI. Note that the increased current has negligible impact on the lithiation and delithiation for the Si electrodes. The dQ/dV plots in Fig. 3a confirm no changes in delithiation potentials. Due to the mitigated side reactions, the higher Coulombic efficiencies (CE) is observed when using higher cycling current (Fig. 3b).

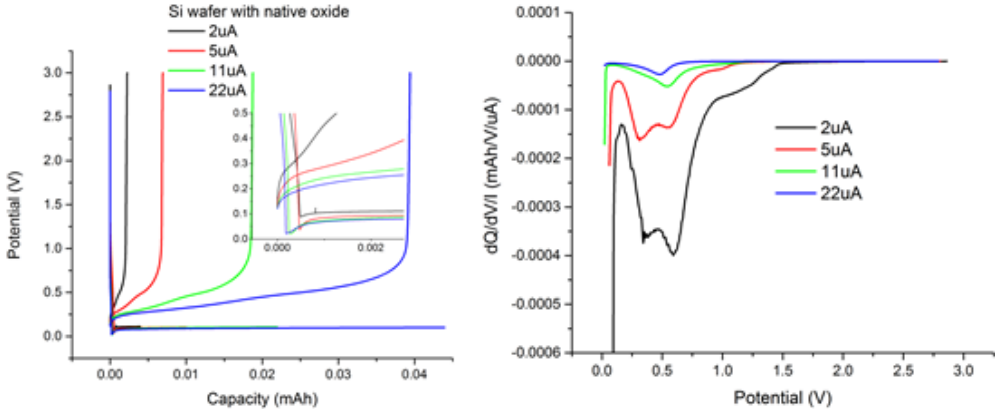

Figure 2. (a) The voltage profiles of the Si electrodes during lithiation. (b) dQ/dV plots of the lithiation process at increased currents.

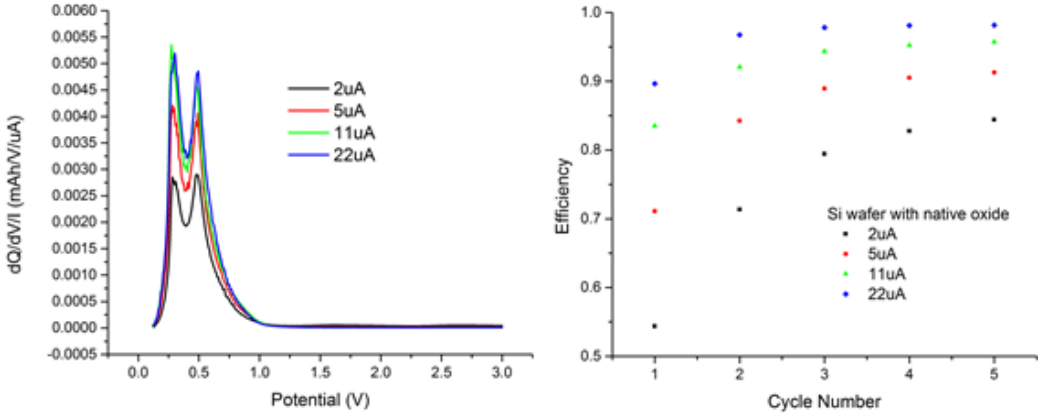

Figure 3. (a) The voltage profiles of the Si electrodes during delithiation. (b) CE as a function of the cycling numbers for Si electrodes at increased cycling currents.

Conclusions

Thanks to the establishment of the standard Si samples, cell fabrication and cycling protocols, we were able to investigate the initial state of the electrolyte reduction process, which has been largely overlooked. The formation of the early-stage SEI determines the interface between the SEI and the electrode surface, which dominates the electrochemical properties of the Si anodes. By defining the early-stage SEI formation, this research clearly shows the impact of cycling current on the electrochemical behavior of the early-stage SEI and the cycling efficiency. Following the strategy, the work in the next quarters will investigate the electrochemistry of the early-stage SEI under different electrolytes and different surface species, with the goal of stabilizing the silicon surface without sacrificing power and energy density.

Materials Standardization - Aging Effects on Thin-Film Si (NREL)

National Renewable Energy Laboratory: Interfacial and Surface Science Group
Kevin Wood, Steve Harvey, and Glenn Teeter

Background

The reactivity of Si anodes causes problems for reproducibility and reliability of Si-based battery systems. Unfortunately, detailed experiments showing how packaging, shipping, and storage of Si thin film anodes effects the electrochemical performance is lacking. Furthermore, it is typically assumed that storing a sample in an Ar-filled glovebox will keep the sample surface relatively unchanged, and thereby lead to reproducible and consistent data sets. During Q1 FY18, we have investigated these assumptions about shipping/storage of potentially reactive battery materials, and have probed the effects of different glovebox ambient environments (and air exposure) on thin film Si samples.

- *Understanding surface reactivity of thin film Si Anode materials*

Results

To investigate the effects of storing Si thin film samples in different gloveboxes, a series of experiments were conceived and executed by SEISta team members. Staff at Oak Ridge National Laboratory (ORNL) made thin film Si (~200-nm) on Cu foil substrates, and distributed samples from the same deposition run to each of the five partner national laboratories. Upon receipt by the different national labs, the thin film samples were opened in gloveboxes and exposed for five days. After this five-day period, the samples from each lab were sealed and shipped to the National Renewable Energy Laboratory (NREL) for surface analysis with x-ray photoelectron spectroscopy (XPS) and time-of-flight secondary-ion mass spectrometry (TOF-SIMS). Each national lab partner also received the materials needed to make three Si-Li coin cell samples. These samples were electrochemically tested in order to establish correlations between the electrochemistry and the surface chemistry.

After receiving samples from the various national labs, a control sample (sent directly to NREL from ORNL and not subjected to a five-day glovebox exposure) was analyzed first, followed by each sample from the five partner labs. Normalized XPS surface spectra are shown in Figure 1 (note that intensities are normalized for clarity). From this data set it is clear that the only new chemical states present on the surface are associated with F, while the Si, O and C chemical states change very little. However, significant differences are observed for the relative atomic concentrations of these species on the surface.

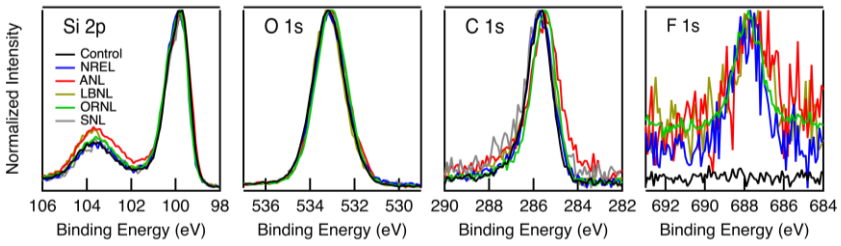

Figure 1. XPS data showing little to no variation in chemical stares present on the surface of the Si thin film samples.

The atomic concentrations for each aged Si thin film are shown in Table I. These data clearly reveal that storing a Si thin film sample in any glovebox environment unsealed causes significant changes to the ratios of surface chemical states. While some boxes appear to be 'cleaner' than others, the relative amount of Si present at the surface always decreases with glovebox aging, while F, C, and O (O in every glovebox but one) increases. Consistent results were observed in the TOF-SIMS surface spectra. Perhaps even more interestingly, storing a Si thin film sample in air caused the surface C and F content to decrease dramatically.

TOF-SIMS and XPS analyses also reveal interesting changes in the aged materials behavior with regard to apparent sputter rates. The sputter-depth scales for each technique were calibrated by correlating the sputter time to a sputter rate obtained from separate measurements on a smooth 100-nm thick SiO_2 reference film on a

Si wafer, as the films in this study were too rough for optical or stylus profilometry measurements. As seen in Fig. 2a, all of the glovebox-aged Si thin film samples sputtered more quickly than the control, giving the appearance that the films thinned with aging. This effect might be due to i) a relative increase in sputter rate that results from changes in film chemistry induced by the different ambient glovebox environments that altered aggregate bond strength in the films; or ii) to the expulsion of water vapor, causing these films to densify[1]. By comparison, data in Fig. 2b shows that it takes longer to sputter through the air-aged film than it does to sputter through the glovebox aged samples or the unaged control. This interesting result might indicate that glovebox-aged films do in fact densify, because the partial pressure of water vapor will be much higher in air than in an Ar glovebox environment, thereby leading to a larger driving force for water expulsion during glovebox storage. However, this result is still far from conclusive and more experiments are needed to understand this phenomenon. In the near future, a simple experiment is planned with sputtered Si films deposited on smooth substrates which will elucidate whether the observed sputter rates are due to changes in the film that affect the sputter rate, or to actual densification of the films.

Table I: Elemental surface analysis after aging Si thin films for 5 days in different gloveboxes across different national laboratories. Controlled unaged and air exposed samples are shown for comparison.

	SNL	NREL	ORNL	ANL	LBNL	Control	Air Exposed
Si	54.04	53.36	51.28	50.86	45.15	56.54	51.73
C	19.19	20.89	20.51	13.53	**22.60**	17.23	12.58
O	26.47	24.64	26.11	**34.94**	31.44	25.93	35.70
F	0.11	1.19	2.21	0.65	0.81	0	0

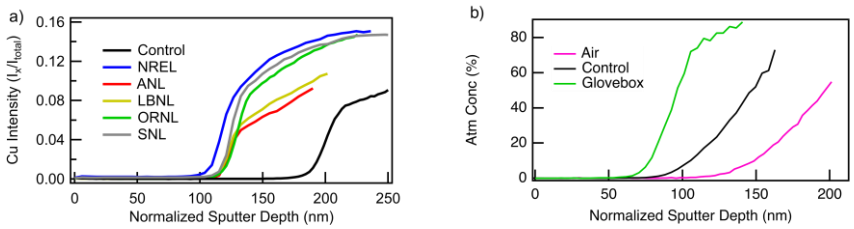

Figure 2. a) TOF-SIMS profile data showing the apparent change in sputter rate of Si thin films samples that have been aged in different glovebox across the 5 national laboratories b) XPS profile data showing the difference between glovebox, control and air exposed Si thin film samples

- *Surface analysis of glovebox stored Si films reveal differences in concentration of C, O and F, but no changes in the functionalities present. Air storage of Si films results in less C and F contamination*
- *Glovebox storage results in the appearance of film densification*
- *Air storage results in the appearance of film expansion*

Conclusions

In summary, XPS and TOF-SIMS measurements have demonstrated that exposure of Si thin films to ambient glovebox environments can lead to significant changes in the surface chemistry and film properties. Unsurprisingly, results show that different gloveboxes lead to different degrees of surface contamination, while the chemical states associated with observed contamination were nearly identical for each glovebox in the study. When comparing glovebox storage to samples stored in air, air-stored films had more O present at the surface, but significantly less C and F. Further analysis of these materials revealed that glovebox storage might lead to a film densification, while air storage might cause the reverse effect. Preliminary analysis of electrochemical data shows a trend suggesting that different surface chemistries indeed affect electrochemical performance. There appears to be a link between the amount of C present on the surface of the sample and the amount of observed capacity obtained in the first half-cycle; higher C content tends to increase capacity.

Difference in properties of Si thin films are observed depending on storage methods. Preliminary analysis of the electrochemical performance suggests a trend between carbon content at the surface and initial capacity.

References

(1) Jansen, F.; Machonkin, M. A.; Palmieri, N.; Kuhman, D. *J. Appl. Phys.* **1987**, *62* (12), 4732–4736.

Model Materials Development and Characterization - Plasma-Synthesized Silicon Nanoparticles

Bertrand Tremolet de Villers, Gregory Pach, Nathan Neale (NREL)

Background

One of NREL's tasks explores plasma-synthesized silicon nanoparticles (Si NPs) as model systems for Li_xSi anodes. Such plasma-prepared Si NPs are valuable since they feature hydrogen-passivated surfaces and a high surface area resulting from their <10 nm diameter that makes them well suited for chemical reactivity studies using Fourier transform infrared (FTIR) spectroscopy and quantitative off-gassing analysis. These reactivity studies are relevant for understanding (1) early-stage SEI layer growth as well as (2) individual SEI component chemical stability. In FY17, we prepared several ~100 mg batches of ~7 nm diameter Si NPs for chemical reactivity studies. Making larger diameter (10–200 nm) Si NPs and at a greater scale (>100 mg) as well as extending chemical reactivity to electrochemical reactivity are key objectives in FY18.

Results

Much of Q1 FY18 was spent evaluating critical project needs and ensuring complementary, value-added studies with the Silicon Deep Dive and external community efforts. We acquired the necessary hardware capabilities to execute that plan, and brought on two new workers (see below) to replace the unexpected loss of a postdoctoral researcher in FY17 (April 2017).

We have continued to work in collaboration with our SEISta partner Prof. Kristin Persson (UC Berkeley) to elucidate the chemical reactivity of our small-diameter Si NPs with electrolyte (EC/$LiPF_6$ and Gen2) via complementary FTIR and DFT studies. As shown in Fig. 1, this study maps the chemical species that form upon reaction of silicon surfaces with Li ion-containing carbonate electrolytes. Model systems with alkoxide and silyl ester groups (suspected chemical species following carbonate electrolyte decomposition) that were intentionally bound to the surface of Si NPs revealed that the silica (SiO_x) formed in the presence of surface-bound alkoxides is relatively robust against dissolution, whereas SiO_x on the surface of Si NPs functionalized with silyl esters is susceptible to chemical attack. Similar studies on different forms of commercial SiO_x found that Fumed SiO_x and 30–50 nm NanoAmor Si (which is primarily SiO_x) are chemically unstable to EC/$LiPF_6$ and Gen2 electrolytes. In contrast, Stöber SiO_x (prepared via a sol-gel process) is virtually unreactive toward these electrolytes. Finally, the reactivity of two types of lithium silicates – Li_2SiO_3 and Li_4SiO_4, prepared at ORNL – evoked as SEI components were additionally compared. Interestingly, we found that Li_2SiO_3 coordinates carbonates while Li_4SiO_4 is relatively unreactive. This work provides insight into the types of chemical species present in the SEI layer that either afford stability or lead to its dissolution. We expect to submit this publication for peer review in Q2 FY18.

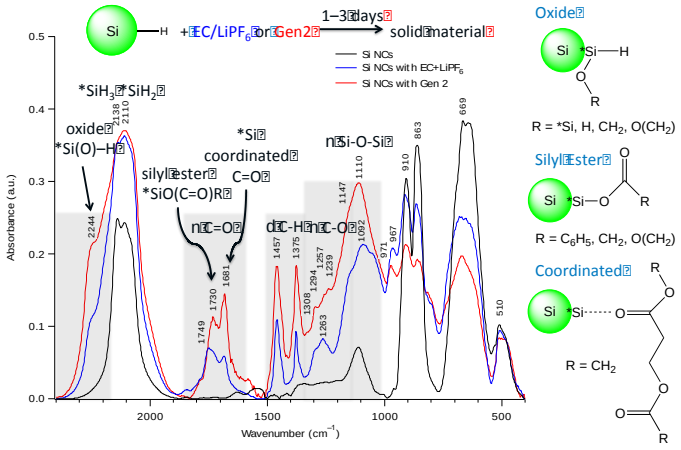

Figure 1. Scaled-up plasma reactor, load-lock collection system, and small diameter (<10 nm) hydrogen-passivated Si NPs.

A complementary gassing study with SEISta partner Gabriel Veith (ORNL) was performed in which the gaseous product from these reactions were quantified using gas chromatrography-mass spectrometry (GC-MS). This ORNL study on NREL's Si NPs as well as in-house prepared lithium silicates and silicon oxides corroborates our FTIR chemical reactivity study. We expect to submit this 2nd publication for peer review also in Q2 FY18.

We have additionally hired a research technician (25%) to speed our progress in developing the protocols to produce larger diameter (10–200 nm) Si NPs and at a greater scale (>100 mg) than is currently available with our existing plasma process. Much work was spent hiring and training the new technician on the plasma production system. In FY17, we acquired a 12-kg cylinder of 100% silane (SiH_4) gas precursor, installed a high flow (500 sccm) silane (SiH_4) gas mass flow controller, and designed and completed testing on a new load-lock collection system capable of collecting gram-scale quantities of Si NPs per reactor run (Fig. 2). We also determined that the plasma power density can be used to tune the Si NPs from amorphous (a-Si) to hydrogenated (a-Si:H) to crystalline (c-Si) that are each expected to provide different anode characteristics in planned FY18 electrochemical reactivity studies. An alternate insert within this load-lock will facilitate up to 5 different samples per reactor run, greatly increasing our throughput as we explore the conditions necessary to produce larger diameter particles. The technician will begin to use these new hardware components to demonstrate a range of Si nanoparticle powder samples from 10–30 nm diameter samples at a scale of 0.2–0.5 g by the end of Q2 FY18.

Figure 2. Scaled-up plasma reactor, load-lock collection system, and small diameter (<10 nm) hydrogen-passivated Si NPs.

Finally, we have brought on a staff scientist (50%) to develop an in operando FTIR-ATR electrochemical apparatus that will allow us to monitor evolution of the SEI on silicon electrodes during electrochemical cycling. We worked extensively with Dr. Phil Ross (LBNL) given his extensive prior work in this area[1,2] to ensure the validity of the design and have ordered the necessary attenuated total reflectance (ATR) hardware for our existing FTIR spectrometer. Pike Technologies was identified as having the best combination of ATR capabilities that will interface with an existing Nicolet 6700 FTIR spectrometer. The necessary Nicolet inert, alignment fixture, electrochemical cell, and ZnSe ATR crystals were purchased. We plan to assemble the new ATR-FTIR setup and conduct preliminary testing with an in operando electrochemical interface in Q2 FY18.

Conclusions

Key findings to date are insight into the types of chemical species present in the SEI layer that either afford stability (alkoxides) or lead to dissolution (silyl ester) of silicon oxides (SiO_x). The role of the type of SiO_x cannot be underestimated, and our studies show that its chemical reactivity (susceptibility to dissolution) is also controlled by the chemical history of the SiO_x. Extending these chemical reactivity studies to monitor electrochemical reactivity using a new in operando ATR-FTIR setup will provide valuable insight into the critical factors affecting electrochemical stability. To do this, an adequate supply of material is required, and we are extending our efforts to prepare Si NP samples at a size and scale more suitable for batter electrode fabrication.

References

1. Shi, F.; Ross, P. N.; Zhao, H.; Liu, G.; Somorjai, G. A.; Komvopoulos, K. *J. Am. Chem. Soc.* 2015, *137*, 3181.
2. Shi, F.; Ross, P. N.; Somorjai, G. A.; Komvopoulos, K. *J. Phys. Chem. C* 2017, *121*, 14476.

Model Materials Development and Characterization – Lithium Silicates Li_xSi_yO

Jaclyn Coyle (UC Boulder), Kevin Zavadil (SNL), Chris Apblett (SNL)

Background

This quarter, the emphasis for the program was turned to generating results in surface analysis that could be shared across testing organizations. To this end, work in establishing a standard sample for thin Si for use in depositing Li_xSi_yO films for characterization of the lithium silicates using ATR-IR. The Q1 milestone of comparable surface analysis was also undertaken using XPS analysis of freshly prepared Si surfaces exposed to environments for various times was performed. In addition, contributions to the bolt for characterizing coin cell data from a standard sample set supplied by NREL and ORNL, and characterization of a standard test cell was performed.

Results

LixSiyO studies

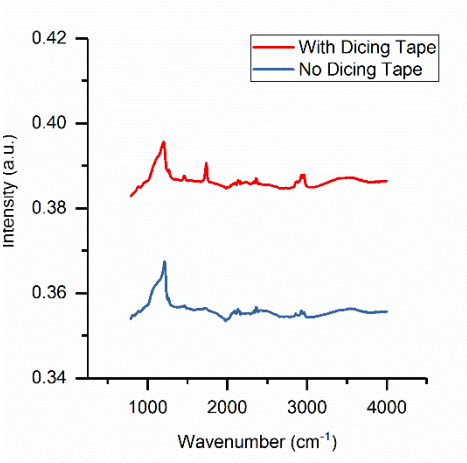

Figure 1: ATR IR spectra of silicon substrate samples with 540nm thick copper and 35nm thick amorphous silicon with and without dicing tape exposure

New samples were developed by depositing a 35nm thick amorphous silicon thin film on top of a 540nm thick Cu layer on a silicon substrate. These samples were also covered in dicing tape and diced into 1cmx1cm squares in order to facilitate more consistent sample size. The tape used to protect the samples from the dicing liquid raised some concerns about how it affects the surface chemistry of the amorphous silicon tin films, especially in comparison with samples that had not been exposed to the dicing tape. To analyze the effect of the dicing tape on the sample surface, ATR IR spectra were taken of samples deposited using the same sample protocols, but with one set getting exposed to the dicing tape while another set was not exposed. Figure 1 shows these ATR IR results. From the ATR IR results, the surfaces of the samples with or without tape have similar chemical compositions. Hydrocarbon peaks appear at the same wavenumber for both sets of samples, just with a higher intensity in the tape sample.
To better understand the nature and evolution of the SEI layer formed prior to any cycling of the silicon anode and how it impacts the performance of the silicon anode, model SEI layers were deposited on clean 50 nm thick silicon thin films using RF

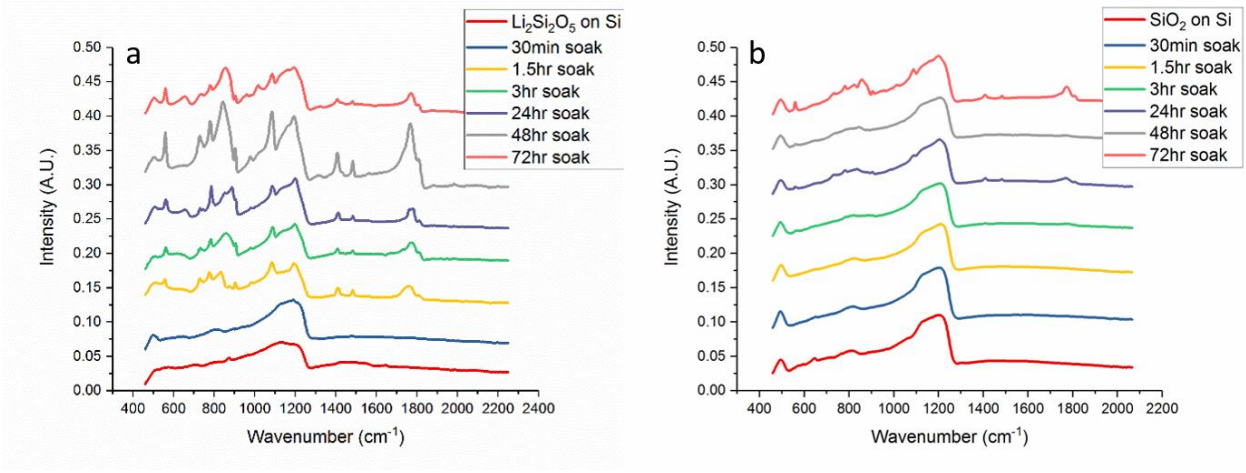

Figure 2: ATR IR spectra of a) $Li_2Si_2O_5$ and b)SiO_2 thin films exposed to electrolyte over time

magnetron co-sputtering. Thin film chemistries from SiO_2 to Li_4SiO_4 were synthesized to model the proposed lithiation of the oxide layer during the first cycle. Model thin films were soaked in 1.2M $LiPF_6$ in EC:EMC 3:7 wt% electrolyte from 30 minutes to 3 days in an inert atmosphere glovebox, removed and rinsed with DMC and studied using ATR IR as seen in Figure 2.

Initial results on these model films after soaking in the electrolyte indicate a dependence on stoichiometry for the time resolved surface reactivity. While electrodes with unlithiated oxide (SiO_2) soaked in electrolyte for up to 24 hours before discernable surface reaction peaks presented in their ATR IR spectra, the electrodes with lithium silicates showed significantly faster appearance of reaction peaks. This could indicate that lithium silicates passivate more quickly against the electrolyte.

Surface Exposure studies

The goal of this study was to determine the surface state of Si electrodes handled in various atmospheres prior to measuring their electrochemical response to alloying with Li. The near-surface composition of 50 nm thick sputtered Si films deposited onto Cu foil current collectors were analyzed using X-ray photoelectron spectroscopy for this purpose. The films were produced *in vacuou* at ORNL, transferred from deposition system to glove box through air, and sealed in a pure argon atmosphere prior to shipping to partner laboratories. Measured atomic percentages of Si, surface contaminants (O and C), and sputter contaminants (N) are listed in Table 1 for films analyzed with minimal storage time (control), storage in an actively gettered glove box (Ar at < 1 ppm O_2 and H_2O) used for Si electrochemical studies, and exposure to the laboratory ambient. Si film storage in a glove box dedicated to Si electrochemistry results in a greater extent of surface reaction as evidenced by the higher surface concentrations of O and C relative to Si when compared to the control film. The corresponding S($2p_{3/2}$) spectra shown in Figure 3 highlight the extent of this surface reaction in the relative intensity of the Si^{4+} peak at 104 eV relative to that of the lower binding energy Si^0. This surface oxide film is enriched in organic constituents, largely aliphatic in nature with evidence of both ether (C-O) and carbonyl (C=O) bonding based on features to higher binding energy of the primary peak. C enrichment is the result of continued reaction of Si with carbonate solvent vapors from the electrolytes used (alkyl carbonates) within the glove box with the post-deposition surface oxide. Traces of F (< 1 at %) have been detected on these stored Si film, likely resulting from trace HF due to decomposition of the supporting electrolyte $LiPF_6$, but readily desorbs with x-ray/electron exposure.

Table-1: XPS Measured Variation in Sputtered Si Surface Composition with Storage in Actively Gettered Argon and after a 15 h Laboratory Air Exposure

	Si (at %)	O (at %)	C (at %)	N (at %)
Storage in Ar	43.9	32.4	23.2	0.5
15 h Air Exposure	42.5	33.3	23.4	0.8
Control*	56.5	25.9	17.2	---

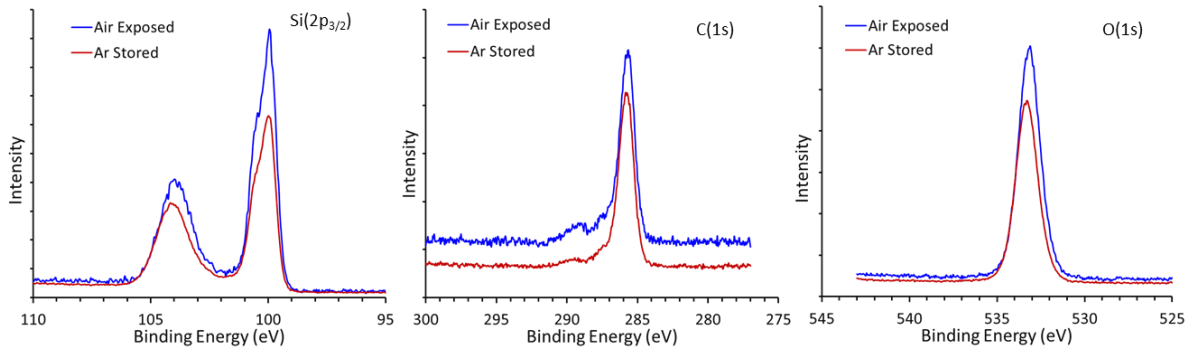

Figure 3. Comparison of Si($2p_{3/2}$), C(1s) and O(1s) lineshapes for sputter deposited Si films stored in an actively gettered Ar glove box and with a 15 hour exposure to laboratory atmopshere.

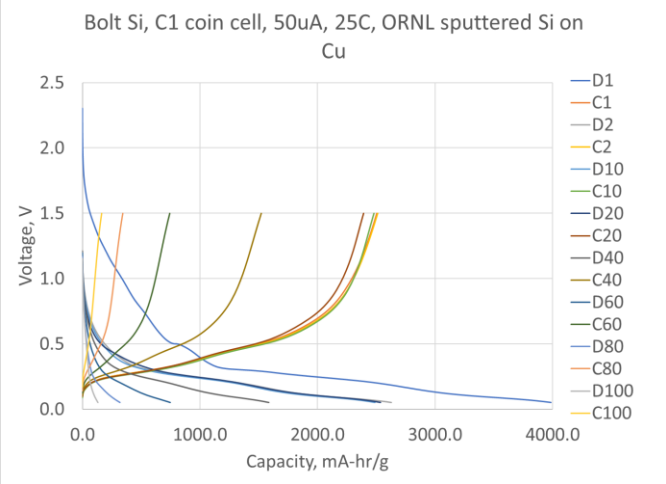

Figure 4: First 100 cycles of 50nm thick Si wafers on Cu foils in coin cells, supplied by ORNL. Results are consistent with other, similar experiments from the other sites.

Bolts and Cell Testing

Rapid screening tests using identical hardware at various facilities, nicknamed "BOLTS", were performed using material supplied from ORNL. These tests were meant to demonstrate reproducibility between the sites in the program to produce similar data. The intent was to compare the first few cycles, but tests were continued on all samples out to 100 cycles for future comparisons. As expected, initial capacities on these thin film (~50nm) thick Si layers produced very high capacities, but quickly faded, with capacities of less than 1000mA-hr/g by cycle 60. Characteristic results from these tests are shown in Figure 4.

An NREL designed test cell was also evaluated using samples supplied from NREL, with a base layer of oxide grown on standard Si samples. These samples also showed consistent behavior to that observed in the literature and from other sites in the consortium, with a first cycle capacity that was fairly low (consistent with single crystal Si cycling), and extremely poor cycle life. This test cell has a relatively high working distance between the working electrode and counterelectrode, which may give rise to polarization resistance, resulting in lower than expected reversibility after first discharge and low capacity. A new cell design based on a standard compression T-Cell design, is being developed.

Conclusions

The use of model silicate systems indicates that surfaces that have differing chemistries on them (SiO_2 vs. $Li_2Si_2O_5$) behave very differently when exposed to electrolyte, with lithiated oxides being much more reactive. However, since all surface oxides must be lithiated to some extent during cycling, the time evolution of these silicates may influence further SEI formation. Surface oxides formed on Si remain sufficiently active and non-passivating resulting in the continued reaction and adsorption of vapor phase organics over time. Attention needs to be paid to the impact these evolving surface films have of Si electrochemistry.

Model Materials Development and Characterization - Individual SEI Components (NREL)

Sang-Don Han

Background

One of NREL's tasks characterizes the physical and electrochemical properties of 'individual' silicon electrolyte interphase (SEI) components, such as Li_xSiO_y, Li_2O, LiF, Li_2CO_3, LiOH, $ROCO_2Li$, ROLi and SiO_xF_y. In addition to electrolyte chemical and electrochemical reactivity analysis of individual SEI components, properties characterization studies of them can provide a strong guidance to aid in the development of new electrolytes, additives and binders to stabilize SEI layer on a silicon anode by identifying beneficial components and providing mechanical explanation of a variety of reactions and phenomena in a SEI. Each individual component was prepared as a thin film, and the prepared films can be characterized using an experimental set-up (Figure-1a) and a variety of analytical equipment including *operando* XPS (X-ray photoelectron spectroscopy), AFM (atomic force microscope), FT-IR (Fourier-transform infrared spectroscopy), SSRM (scanning spreading resistance microscopy) and TOIF-SIMS (time-of-flight secondary ion mass spectrometry).

Results

The thin film samples were prepared by Radio Frequency (RF) magnetron sputtering (13.56 MHz) in an argon-filled inert atmosphere glovebox (<0.5 ppm of H_2O and <0.5 ppm of O_2). A central target was placed 8 cm away from a Si wafer substrate, while another off-axis target was placed 12 cm from the substrate. Ar (99.999 % purity) gas was introduced in a chamber to generate plasma at a constant pressure, and the temperature (up to 270 ºC) was controlled to induce changes in crystallinity degree of a film. Different RF power was applied on target to adjust the film composition. In particular, oxygen concentration in a film can be varied by several ways including control of a distance between the target and the substrate or increase of deposition pressure. A uniform film or a combinatorial film can be prepared by rotating the substrate or keeping it still. The sputtered Li film (as a Li source for electrochemical tests) was added before sputtering an individual component thin film for *operando* XPS analysis. In addition, the reference thin film prepared with well-studied highly stable and relatively conductive $LiAlF_4$ was employed to check the reliability of experimental set-up and to compare the properties of $LiAlF_4$ with those of individual SEI components. All prepared thin films were (partially) covered with additional Cu or Ni thin film to prevent each individual component thin film from further possible reactions and to make metal contacts for electrochemical properties measurements (Figure-1b and -1c).

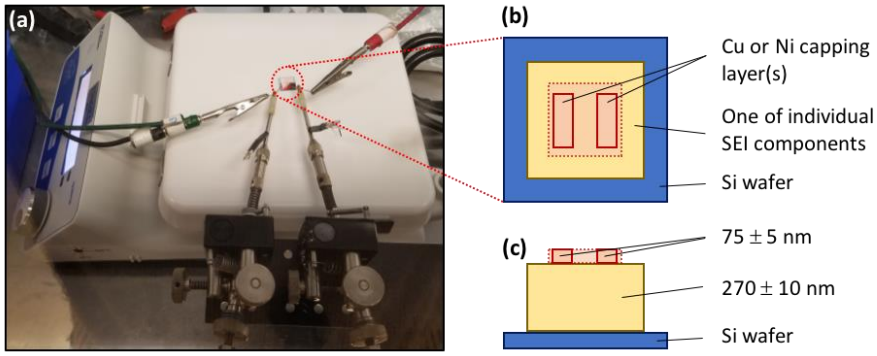

Figure-1: (a) Experimental set-up for physical and electrochemical properties analysis. Schematic (b) top-view and (c) cross-sectional images of thin films formed on a Si wafer (blue square region). Thin films of one of SEI components and Cu (as a capping layer) were sequentially deposited in the yellow and red square regions, respectively.

The physical and electrochemical properties analysis of prepared samples was performed by contacting one of pin-point probes to a Si wafer (actually native SiO_2 on a Si wafer, blue square region in Figure-1b) and another probe to a Cu or Ni layer (red-dot square region in Figure-1b). It is noteworthy that native SiO_2 is formed on the surface of a Si wafer, but its thickness is around 2-3 nm that may be negligible in our measurements.[1] To remove a potential issue, however, additional samples with paired Cu or Ni array (red square regions in Figure-1b) were prepared, and their properties were characterized by contacting one of probes to one of paired Cu or Ni array and another probe to another Cu or Ni array. Figure-2 shows the Nyquist plots of reference and one of individual component thin films ($LiAlF_4$ or Li_2O | Cu or Ni as a capping layer) on a Si wafer at room temperature. Only one semicircular arc for each prepared thin film was observed due to the ionic conduction in each component. These Nyquist plots can determine ionic conductivity of individual components. For example, $LiAlF_4$ with the thickness (L (cm)) of 79 x 10^{-7} cm was deposited on a Si wafer by using physical mask as shown by yellow square region in Figure-1b. The area (A (cm^2)) of red dot square region of a Cu capping layer in Figure-1b is 1 cm^2. Ionic resistance (R (Ω)) of $LiAlF_4$ was measured between a Si wafer and a Cu capping layer, and the ionic conductivity (σ_i (S cm^{-1})) was calculated from below equation to be 1.3 x 10^{-9} S cm^{-1}:

$$\sigma_i = \frac{L}{R \cdot A}$$

This value is lower than the previous report ($3.5 \pm 0.5 \times 10^{-8}$ S cm^{-1}),[2] but at least the typical plot of a thin film in the similar sample configuration is observed as shown in previous research,[3,4] which indicates the experimental set-up is reliable for further measurements. Therefore, continuous effort has been devoted to address potential issues in sample preparation and to develop better sample configuration for more precise and reproducible data.

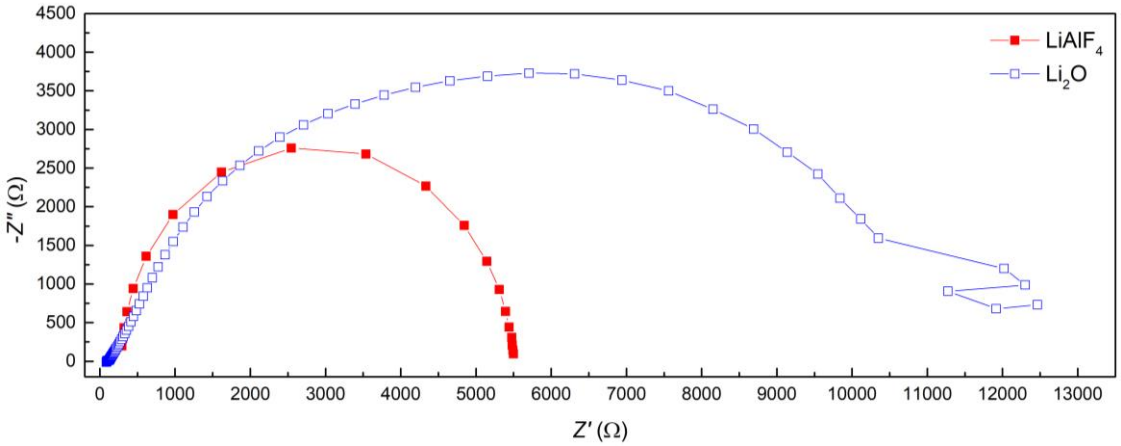

Figure-2: Nyquist plots of $LiAlF_4$ and Li_2O thin films obtained at 25 °C.

Sample Preparation Approach: For additional experiments with more reactive SEI components (e.g., Li_xSiO_y, LiF and Li_2O) a sample was newly prepared with an additional ion-blocking Cu thin film between a Si wafer and a SEI component thin film to prevent potential Li^+ ion diffusion or possible chemical/electrochemical reactions. Figure-3 represents XPS in-depth analysis of the prepared sample, Cu (as an ion-blocking layer) on a Si wafer | Li_xSiO_y | Cu. As expected, the Li_xSiO_y thin film with a thickness of 100 nm is observed from around 100 nm depth, which is sandwiched between two Cu thin films, but unexpected Li_xO layer was detected on the top of the sample, which may be attributed to a preparation method failure or cross contamination of used materials. In addition, most prepared samples of Cu on a Si wafer | $LiAlF_4$ or LiF or Li_2O or Li_xSiO_y | Cu show short-circuit behaviors for impedance measurements, which can be attributed to surface roughness of Cu. Instead of Cu, thus, a Ni or Pt thin film will be sputtered as an ion-blocking layer with careful sample preparation procedures.[3]

Besides addition of an ion-blocking layer to a sample, the interdigitated platinum electrodes, which are composed of two interdigitated electrodes with two connection tracks (all made of platinum) on a glass substrate, will be

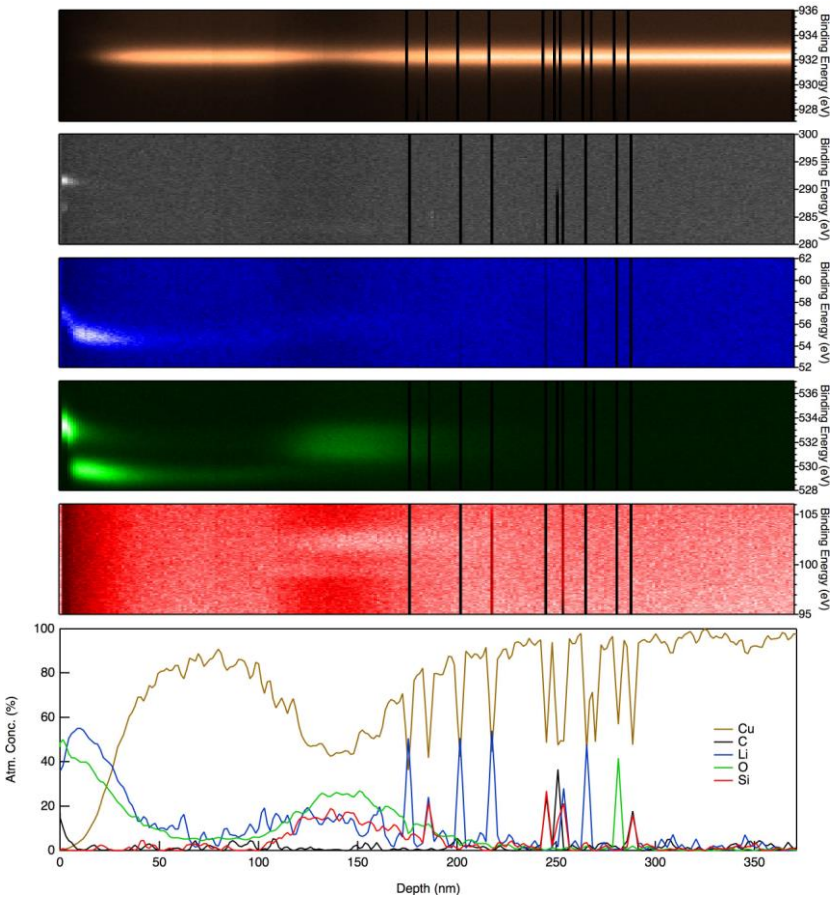

Figure-3: XPS in-depth analysis of the prepared sample, Cu (as an ion-blocking layer) on a Si wafer | LixSiOy | Cu.

employed in future sample preparation to enhance sensitivity and detection limits in electrochemical measurements.[4]

Conclusions

Additional Characterization Techniques and Equipment: Utilizing the experimental set-up, the physical property (Li^+ ion diffusion coefficient using the Arrhenius law) of a newly developed sample will be determined by collecting impedance data with varying temperatures. Complementary experiments using XPS has been designed to probe both chemical composition and electronic/ionic conductivity at the same time. This novel technique uses sample biasing to measure binding energy shifts, which came be related to either ionic or electronic conductivity. Within the last quarter these experiments have been initiated. To add additional characterization of the local electronic structure and resistance of individual SEI components, which are important to understand SEI heterogeneity laterally and vertically to assess stratification of components, a SSRM will be used. The hardness of SEI constituents can be studied by AFM force distance curves and nanoindentation.

References

1. S.-B. Son *et al.*, *ACS Appl. Mater. Interfaces* **2017**, *9*, 40143-40150.
2. J. Xie *et al.*, *ACS Nano* **2017**, *11*, 7019-7027.
3. C. Li *et al.*, *Adv. Funct. Mater.* **2012**, *22*, 1145-1149.
4. M. Sato *et al.*, *Electrochem. Commun.* **2018**, *87*, 31-34.

Model Materials Development and Characterization - Lithium Silicide films

Yun Xu, Kevin Wood, Glenn Teeter, Caleb Stetson, Andriy Zakutayev (NREL)

Background

The goal of this work was to study the properties and reactivity of lithium silicide thin films. The advantage of using lithium silicide prepared by physical or chemical methods is that the measurements of its properties are not effected by SEI, which is inevitable when the lithium silicide is prepared by electrochemical potential driven lithiation of silicon. The thin film configuration of lithium silicide samples also makes the study of the surface reactivity easier and more accurate compared to the samples prepared in particles form

Published studies of lithium silicide are much more rare compared to papers on silicon or other lithium compound. This is mainly due to high reactivity of the lithium silicide. The few available previous studies on lithium silicide have all been focused on samples prepared by mechanical milling of lithium and silicon, or by electrochemical potential driven lithiation of silicon.[1, 2] However, no reports on physically or chemically synthesized lithium silicide thin film without oxygen have been made. The only reported "lithium silicide" thin film has an oxygen contamination of 10 at%. [3]

Results

Synthesis result

Lithium silicide thin films were obtained from Li/Si bilayers deposited through a combination technique of evaporation of Li and sputtering or Si. Si was sputtered with power of 90W on a 2 inch target. Ar process gas with processing pressure of 5 x 10^{-3} Torr was used during deposition. Lithium foil was used as evaporation source for lithium. Base pressure of evaporation was 6 x 10^{-8} Torr. The lithium silicide then was formed by inter-diffusion between lithium and silicon layers. Various thicknesses of lithium (0, 100, 200, 260 nm) were deposited on 50 nm silicon, in order to get lithium silicide with different degrees of lithiation. This procedure is very different than co-sputtering Li and Si we worked in the past, and is expected to lead to lower oxygen contamination of the lithium silicide thin films.

Chemical composition

To evaluate chemical composition of the lithium silicide thin films, x-ray photoelectron spectra (XPS) were collected for a film with 200nm of lithium on top of 50nm silicon film. The results are shown in Figure 1. The film shows a gradient of lithium/silicon in the depth direction and negligible concentration of oxygen in the bulk of the film. Lithium concentration gradually decreases from surface to bulk, while the silicon gradually increases in this direction. The lithium-silicon ratio ranges from Li_2Si-LiSi. From the binding energy of Si 2p, at the depth of around 50-150nm, where there is negligible oxygen, Si has a low binding energy of around 98 eV, indicating the formation of lithium silicide. Despite the sample was stored in the glovebox (3 days), surface oxygen contamination appears inevitable. It is also interesting to note that lithium silicide is so reactive that it even reacted with the native oxide layer on the surface of copper foil substrate. The observed surface contamination of PF_6 is likely from the glovebox where heavy electrolyte operations are performed. Due the roughness of copper substrate, it is difficult to obtain the accurate thickness of thin film from these measurements.

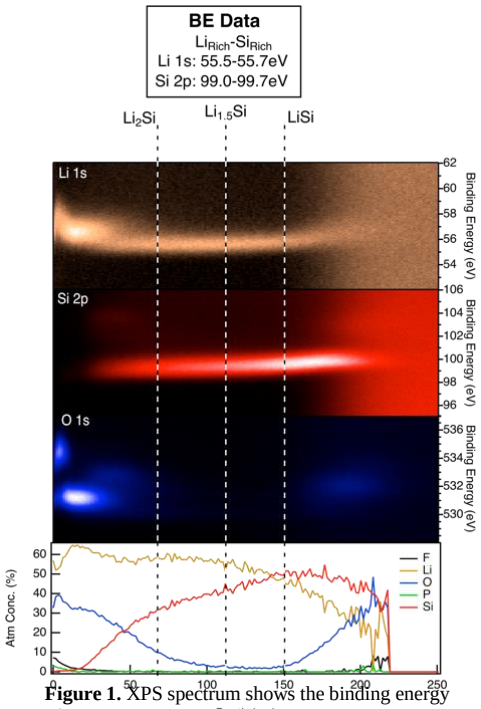

Figure 1. XPS spectrum shows the binding energy of Li, Si, O changes along the depth direction. Bottom figure shows the composition gradient changes along the depth direction.

Electrochemical properties

To study the electrochemical properties of lithium silicide, coin cells were fabricated by assembling the deposited thin film against lithium foil. The electrolyte was 1M LiPF6 in a 1:1 (volume) ethylene carbonate (EC) and dimethyl carbonate (DMC) solution. Lithium silicide thin films were delithiated first and silicon thin films were lithiated first. The voltage profiles of cells made with different lithium silicide films, are shown in Figure

2a. The thicker the lithium film is, the lower the OCV is, but the CV curves did not exhibit plateau. Figure 2b is voltage profiles of 50nm silicon thin film without any lithium in them, and litheated first. The voltage profile of silicon thin film showed plateau for both charge and discharge profiles. Compared to the delitheated lithium silicide film, the lithated silicon thin film showed a more obvious plateau because the lithium silicide film had a gradient of lithium concentration in the depth direction.

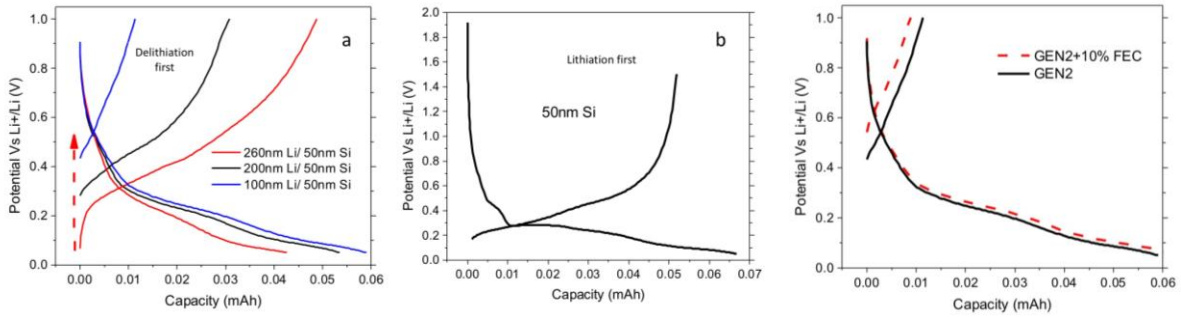

Figure 2. a) Voltage profiles (delithiation first) of lithium silicide thin films prepared from bilayers with different thickness of lithium on top of fixed thickness of silicon; b) voltage profiles of silicon thin film (lithiation first); (c) comparison of voltage profiles for cells cycled in different electrolyte (with and without FEC additive)

Electrolyte stability

The influence of electrolyte composition on the voltage profiles was studied in this work, for electrolytes both with and without FEC. Such studies are important, because when silicon expands upon lithiation and SEI breaks down, the exposed surface would be lithium silicide. As shown in Figure 4, increase of OCV was observed when FEC was added to the electrolyte. This systematic increase of OCV can be attributed to accumulation of electrolyte reduction products on the surface of lithium silicide electrodes. Indeed, there has been a computation study of the reactivity of FEC and lithium silicide, claiming that FEC reacts with lithium silicide extremely fast, resulting in formation of CO_2, F, CH_2CHO or CO_2, F, and OCH_2CHO.[4] To experimentally verify this mechanism, our future work would be focused on measuring the reduction products of the electrolyte on lithium silicide surface with different degrees of lithiation.

Impedance measurement by probe contacting method

To evaluate the electrical conductivity of lithium silicide thin films, we attempted impedance spectroscopy measurements. A silicon substrate was used in this case in order to obtain a smooth interface. Lithium was then evaporated onto silicon wafer, followed by sputtering two titanium pads as electronic contact. Impedance data was collected at room temperature in a frequency range of 500KHz to 5Hz. The sample showed pure resistor behavior when directly probing the lithium silicide surface, while it showed two impedance semi-circle when probing the surface of Titanium pads. This may be related to the interface reaction between the titanium and lithium silicide. Next steps would be to replace Ti pads with less reactive material. We also plan to deposit lithium silicide bilayers as described above on metal-coated Si wafer supports, to directly compare the impedance results with the electrochemical characterization results

Conclusions

Lithium silicide thin films with negligible oxygen concentration in the bulk have been prepared for the first time from Li/Si bilayers deposited by a combination of Li evaporation and Si sputtering. Lithium silicide with different lithiation degrees showed different OCVs and voltage profiles did not show obvious phase transition due to the solid solution nature of thin film. Chemical reaction of lithium silicide with FEC additive in electrolyte has been observed by increase OCV of the coin cells prior to delithiation. Impedance spectroscopy has been applied to measure the resistance, and it was found that lithium silicide is very electronic conductive.

References

1. K. Ogata, Nature Communications 5, 3217 (2014).
2. X. H. Nature Nanotechnology 7, 749 (2012).
3. Strau, E. RSC Advances 5 (10), 7192-7195 (2015).
4. J. M. Physical Chemistry Chemical Physics 16 (32), 17091-17098 (2014).

Model Materials Development and Characterization – Bulk Lithium Silicide (ANL)

J. Vaughey (Argonne National Laboratory)

Background

The focus of the SEISta program is to develop an in-depth understanding of underlying reactions, conditions, and sample history that all combine to influence the properties of the surface electrolyte interface (SEI). As the primary protective layer in a lithium-ion energy storage system, understanding the SEI layer is critical to defining and understanding various failure mechanisms that lead to performance degradation. For silicon-based systems in particular, an understanding of the SEI layer is critical as many of the hypothesized causes of capacity fade and poor coulombic efficiency are, at their core, derived from an unstable SEI layer [1]. Previous published (theoretical, experimental) work had shown that on the first charge the surface silica passivation layer converted to the lithium-ion conductor Li_4SiO_4 [2,3]. We were able to show that in the cell environment, that this phase was metastable and in fact reacted with the electrolyte (with loss of lithia) to form the poor lithium-ion conducting phase Li_2SiO_3 [4]. The reactivity of the surface of the silicon electrode is key to understanding the growth and stability of the SEI layer. In our present efforts we have focused on identifying, synthesizing, and characterizing materials that are representative of the silicon electrodes surface at various states of charge. Working with the characterization teams, we have (1) synthesized and shared various lithium silicide materials, and (2) evaluated Si thin films as part of a baseline round robin study. This project addresses the stability of the charged electrode and the associated problems of the reactivity of the active material towards the constituents of the cell. This buildup of reaction products contributes to the fundamental problem of cycle to cycle instability associated with SEI layer.

Results

We have continued our participation in the round robin thin film effort organized by ORNL to assess the ability to create a baseline Si film electrode. In these round robin efforts, we submitted ANL-created Si films to the program and evaluated common films created at ORNL. The capability to make PVD Si films for the program at Argonne is derived from the need to have Si-coated sensors for our EQCM studies. In the initial studies, the ANL created films were evaluated and compared to the other labs. Initial results found the ANL films exhibited a higher capacity than anticipated based on the amount of silicon deposited. The majority of the extra capacity was found to occur at a potential of approximately ~1.2V (vs Li). ORNL was able to show that offsetting the 1st cycle data made a good approximation to the other labs results, indicating the reaction to produce the extra capacity may be exterior to the active silicon particles. Looking at the history of the samples studied indicated that either the films were contaminated in the PVD chamber (Bi target in chamber) or the copper foils were partly oxidized by the process. Literature analysis and further XPS studies led us to believe that the most likely impurity were phases on the underlying copper foil (i.e. Cu_2O). Literature values had indicated Cu_2O decomposes around 1.3V (vs Li) while Bi lithiates (to Li_3Bi) around 1V. Subsequent round robin studies did not show this extra capacity and data fell in line with the other test centers.

With Baris Key and Binghong Han, I have been synthesizing a variety of lithiated silicides for evaluation in order to assess their stability and reactivity in the full cell environment. Initial work has focused on the phases Li_7Si_3, which is associated with voltage of approximately 350 mV (vs Li) and $Li_{13}Si_4$ (50 mV vs Li) [5]. Phase diagram and crucible studies were performed and conditions and materials identified to synthesize samples. The chosen process was found to be a stoichiometric mixture of Si and Li, Ta crucibles, with a heating ramp to 750 °C, followed by a one hour hold, all under an argon atmosphere. Initial samples were near single phase Li_7Si_3 by powder X-ray diffraction and ^{29}Si NMR. For the phase Li_7Si_3, once a reliable method was identified, the effort was re-focused on a scale up synthesis of crystalline samples with an evaluation of its stability allowing for team members to use these charged electrode model compounds for continued studies. In association with the round robin study, samples were evaluated with regard to their stability in the box atmosphere and over time. Previous samples stored under vacuum appeared to be stable. Powder X-ray

diffraction, Raman, and MAS-NMR studies indicated that the samples appear to react with trace quantities of moisture (air) to produce a diamagnetic lithium phase (by NMR) and, by charge balance, oxidized silicides. Additional studies on an whether the oxidation, which produces a new passivation coating on the lithiated silicon, contains amorphous silica, proton/hydride inclusion, or elemental silicon as the end product of the subtle oxidation are underway.

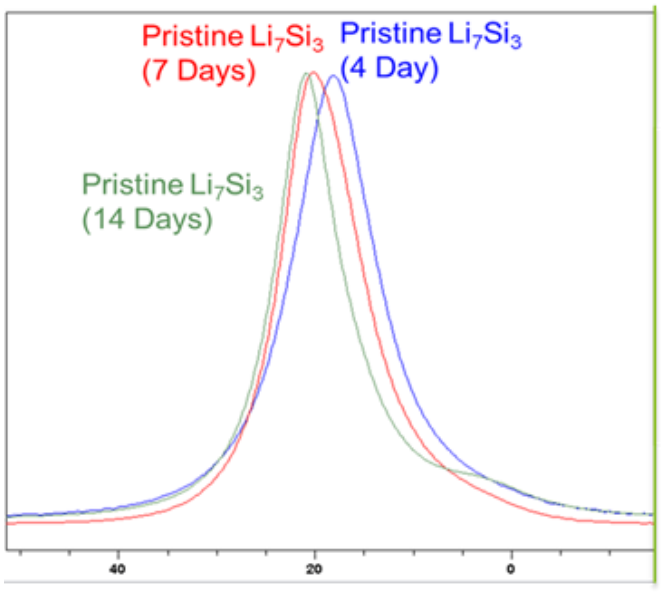

Figure 1. ^{7}Li MAS-NMR spectra of a Li_7Si_3 sample stored in a Ar-glovebox. On standing, the main peak moves to the left indicative of sample oxidation. After 14 days the peak stops moving possibly related to establishment of a surface passivation coating or a more oxidized silicide.

Conclusions

The SEI layer of silicon is a complex, every changing component of the lithium-based electrochemical cell. Our effort within the program is concerned with developing an understanding of how the silicon (Li_xSi, Li_xSiO_y) species within the electrode interacts with their environment to produce the components observed within the SEI layer. We have synthesized and scaled up single phase compounds that represent the silicon electrode at various states of charge and using MAS-NMR, Raman, and X-ray diffraction started assessing the types of phases formed at the electrode-electrolyte interface as a function of state of charge.

References

[1] Alison L. Michan, G. Divitini, A. J. Pell, M. Leskes, C. Ducati, Clare P. Grey *J. Am. Chem. Soc*., **138**, 7918−7931 (2016)

[2] Sung-Yup Kim, Yue Qi *J. Electrochem. Soc*, **161**, F3137-F3143 (2014).

[3] Bertrand Philippe, R. Dedryvère, M. Gorgoi, H. Rensmo, Danielle Gonbeau, Kristina Edström *Chem. Mater*., **25**, 394−404 (2013).

[4] Aude A. Hubaud, Z.Z. Yang, D. J. Schroeder, Fulya Dogan, L. Trahey, J. T. Vaughey *J. Power Sources* **282**, 639-644 (2015).

[5] C. J. Wen, R. Huggins *J. Solid State Chemistry*, **37**, 271-278 (1981).

SEI Characterization – Understanding the Si SEI from Coupled Molecular Dynamics – First-principles Calculations (UC Berkeley)

Kristin Persson (UC Berkeley)

Background

Understanding the underlying atomistic mechanisms for the Si anode performance is crucial for improving current materials and incorporating higher capacity anodes into future, improved lithium ion technology. Our examination of the Si anode reactions includes modeling of the solvation structures within the bulk electrolyte, bulk anode, and the interfacial reactions. We first investigate candidate reaction pathways by examining the solvation structure of the Li ion and electrolyte molecules at the bulk electrolyte and at the interface. For that, we utilize theoretical and computational approach including the DFT calculation and molecular dynamics simulation methods.

A commonly used electrolyte recipe for the Si anode system is the ethylene carbonate (EC) with additional 5%~20% fluoroethylene carbonate (FEC), mixed with 1 M $LiPF_6$ lithium salt. As part of the effort, we will elucidate the solvation structure, reduction reactions and the SEI formation process of the electrolyte system in this electrolyte. Furthermore, classical molecular dynamic simulations (MD) are used to characterize the solvation structure, self-diffusion coefficient, and other macroscopic properties of the electrolytes (1 M LiPF6 in EC, EC/EMC, and EC/FEC) in their bulk phase and at the interface, which help understand the SEI formation reactions. The calculated property results are compared with the experimental results to validate the potentials for MD simulation. With the calculated solvation structure, the 6-31++g* level quantum chemical calculation is conducted to get the IR spectrum result. The calculated and experiment-obtained IR spectrum are compared to assign peaks with certain species, from which the solvation structure can be deciphered accordingly.

Current research focuses on the formation of the SEI and its constituents, but fewer publications exist on modifications to the bulk Si. Dopants and alloys can be an effective way of modifying electrochemical properties. Literature reports show some experimental efforts on Si-Sn, Si-Sn-C, and Si-Sn-O alloy systems.[1] In the Si-Sn alloys, high initial coulombic efficiency (up to 95%) was observed as well as good cycling capability.[2] Our efforts will focus on identifying systems with higher Li mobility and lower volumetric expansion.

Results

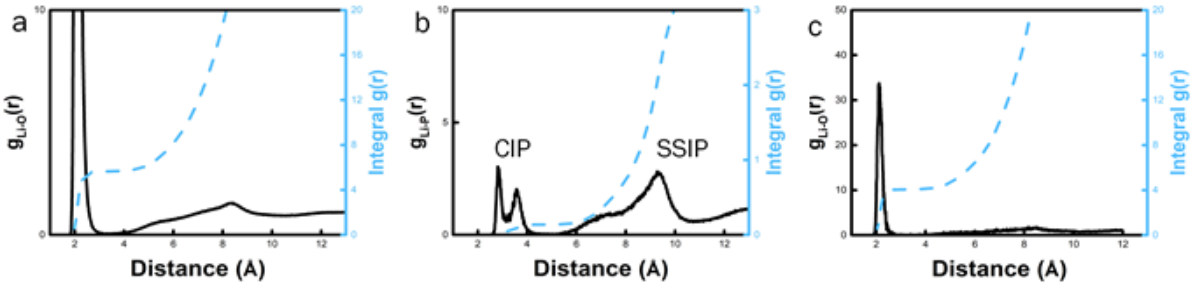

Figure 1. The a) Li-O, and b) Li-P radial distribution functions (RDFs). c) Li-O RDF with modified OPLS parameters.

To achieve rapid evaluations of the bulk electrolyte properties, pure EC was calculated through classical MD using OPLS and GAFF potentials. For the two sets of potential adopted, OPLS gives better enthalpy and relative permittivity results while GAFF underestimates the permittivity. Thus, the OPLS potential is selected for the following simulation process. Subsequently, 5 ns of NVT run of MD simulation were conducted for 1 M $LiPF_6$ in EC. According to the radial distribution functions (RDFs), the total coordination number (CN) for Li ion is around 5.64 (Figure 1a). Two basic solvation structures are observed, one is solvent-separated ion pair (SSIP)

and one is contact ion pair (CIP). For the Li RDFs, the CN for P is 0.14 (Figure 1b), indicating a CIP ratio of 14%. Furthermore, there also exists a small portion of aggregate solvates (AGGs). Benchmarking with *ab initio* molecular dynamics (AIMD)[3] and experimental[4] results, the CN for Li in EC is obtained as 4. A series of OPLS parameters[5] were tested and screened. From a set of parameters with modified Li^+ pair potential and EC charges, a CN of 4.06 (Figure 1c) was obtained, and we subsequently selected the parameters to employ in the future, in order to get an accurate CN of around 4 in accordance with the AIMD and experimental results.

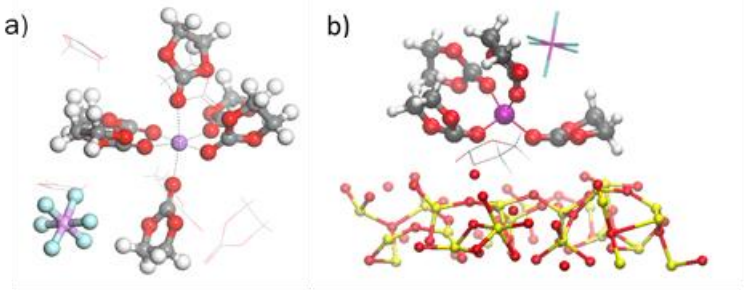

Figure 2. Structures of EC molecules around a Li ion a) in bulk and b) at interface

Interfacial properties of ions/electrolyte molecules of $LiPF_6$/EC at Si anode at the initial charging step is being studied via constant potential method (CPM) with classical MD to overcome the limit of conventional fixed charge method. At the initial state of charging, a Si anode is modeled with a crystalline structure and amorphous native silicon oxide top layer. We first investigated the solvation structure of electrolyte molecules close to the interface. 1 M $LiPF_6$ in EC with OPLS force field is employed as the electrolyte, and neat crystalline Si with/without native silicon oxide layer as the anode. We found change in solvation structure of EC molecules near Li ion from bulk to interface, with CN ~ 6 to ~ 4 (Figure 2).

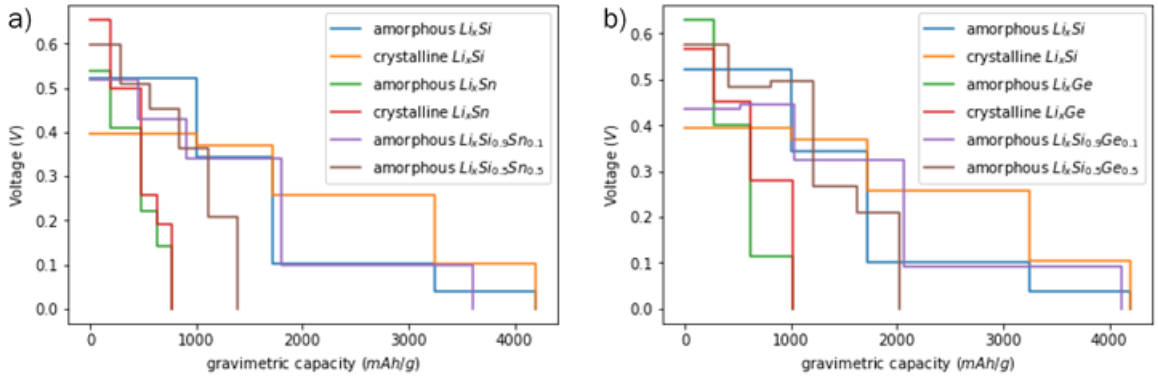

Figure 3: Voltage profiles for a) Si-Sn b) Si-Ge alloy systems

Within the bulk anode, investigations into Si alloys have been initiated. The first two alloy systems investigated were the Si-Ge and Si-Sn alloys, for their similar valency to Si. Voltage profiles for the Si-Ge system (Figure 3a) show comparable lithiation voltages vs Li/Li+, with a slightly lower potential in $Li_xSi_{0.9}Ge_{0.1}$ and higher potential in $Li_xSi_{0.5}Ge_{0.5}$. Figure 3b shows the lithiation potentials for the Si-Sn alloys investigated. Like the Si-Ge system, the system exhibits similar trends: similar potentials with a marginal potential decrease in the 90-10 alloy and greater (by ~0.1V) in 50% Sn alloy.

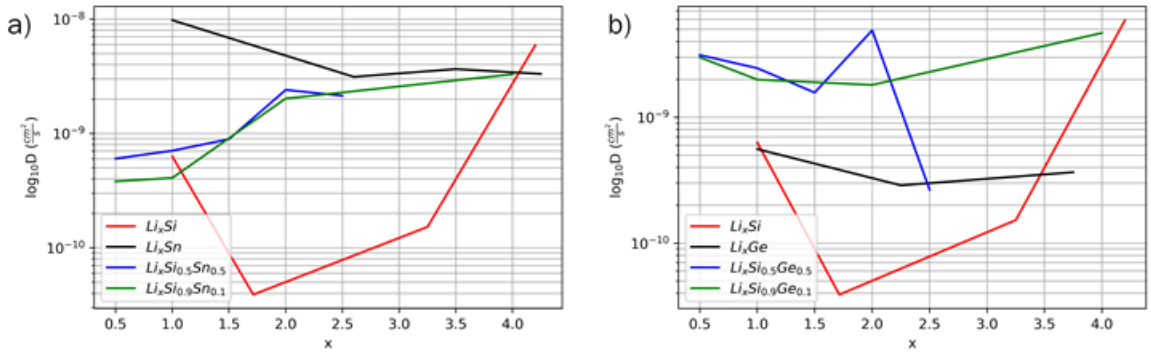

Figure 4: Diffusivities as a function of composition for a) Si-Sn b) Si-Ge alloy systems

Li self-diffusion in the Sn alloy systems (Figure 4a) is promising, showing an order magnitude greater values as compared to pure Si (~10^{-9}-10^{-10}). Due to the higher Li mobility in Li_xSn, the Li mobility in the alloys is greater than in the Si anode. Interestingly, the difference between the 50-50 and 90-10 Si/Sn diffusivities is small, indicating that a threshold Sn content is enough to establish fast Li diffusion. The Li diffusivities are also increased in the Ge alloys (Figure 4b), however in this system, the diffusivity of the alloy is greater than the base materials, Ge and Si, indicating an interesting alloying effect. In both systems, diffusivity is increased for even 10% alloying suggesting that introducing a secondary element to Si shows promise. Work to understand the origins of the increased Li transport in Si/Ge alloy and mechanism for high impact at only 10% alloying is ongoing.

Conclusions

1. We tested the solvation structure of EC molecules in electrolyte around a Li ion in bulk and at the interface, and find the suitable force fields of electrolyte molecules to make the MD results comparable to the AIMD and experimental ones with solvation structure.
2. Si-based alloys, shows better performance, both in terms of lithiation potentials and Li ion diffusivity: with Si/Ge slightly better than Si/Sn.

References

[1] Zhao, X.; Schreiber, M. T.; MacEachern, L.; Sanderson, R. J.; Dunlap, R. A.; Obrovac, M. N. Combinatorial Study of the Si-Sn-O System as Negative Electrode Materials in Li-Ion Cells. *J. Electrochem. Soc.* **2015**, *163*(2), A203–A209.

[2] Hatchard, T. D.; Obrovac, M. N.; Dahn, J. R. A Comparison of the Reactions of the SiSn, SiAg, and SiZn Binary Systems with L3i. *J. Electrochem. Soc.* **2006**, *153*(2), A282-287.

[3] Ganesh, P.; Jiang, De-en; Kent, P. R. C. Accurate Static and Dynamic Properties of Liquid Electrolytes for Li-Ion Batteries from ab initio Molecular Dynamics. *J. Phys. Chem. B* **2011**, *115*(12), 3085–3090.

[4] Kameda, Y; Umebayashi, Y; Takeuchi, M; Wahab, A. B.; Fukuda, S.; Ishiguro, S.; Sasaki, M; Amo, Y; Usuki T. Solvation Structure of Li^+ in Concentrated $LiPF_6$–Propylene Carbonate Solutions. *J. Phys. Chem. B* **2007**, *111*(22), 6104-6109.

[5] Chaudhari, M. I.; Nair, J. R.; Pratt, L. R.; Soto, F. A.; Balbuena, P. B.; Rempe. S. B. Scaling Atomic Partial Charges of Carbonate Solvents for Lithium Ion Solvation and Diffusion. *J. Chem. Theory Comput.* **2016**, *12*(12), 5709−5718.

SEI Characterization – Oxide Coated Silicon Wafers

Atetegeb M. Haregewoin, Ivana Hasa, Liang Zhang, Jinghua Guo, Philip N. Ross and Robert Kostecki (LBNL)

Background

The interfacial properties of Si anode in organic based electrolytes are affected by the presence of native oxide surface layer. The role and the effect of the oxide layer is still uncertain and not fully understood. In fact, it has been reported that the presence of SiO_2 lead to the conversion of surface oxide to Li_2O and Si or to $LiSi_xO_y$ [2,3]. Contrary to this, Larcher et al. [1] reported that even though the conversion of SiO_2 to Li_2O and Si is thermodynamically favorable (ΔE_0 = 0.19 V vs Li^+/Li), overpotentials of about 1 V are necessary to trigger these types of conversion reactions. Hence, given that thermodynamically the conversion reaction is expected to occur, it is important to study whether the conversion reaction is also kinetically favored. Moreover, it should be considered that SiO_2 could represent a barrier for bulk lithiation, leading to an increase of the interfacial charge transfer impedance and hindering the complete lithiation of the underlying silicon.

Our effort in the last two quarters has focused on the role of the native oxide in the interfacial chemistry of Si anodes using model electrode systems. In the fourth quarter of FY17, we selected silicon oxide films thermally grown on Si wafers as model systems and studied their electrochemical behavior to understand the effect of the thickness of the oxide films on the electrochemical performance and interfacial property of Si anodes. We purchased B-doped Si(100) wafer with different oxide thicknesses, native oxide (2nm), 100 nm and 300 nm, from a commercial vendor. In the first quarter of FY18, we continued to work on these model electrodes. Detailed electrochemical analysis and various spectroscopic and microscopic techniques have been applied to study the change in the interfacial phenomenon at the Si/electrolyte, oxide/electrolyte and Si/oxide/electrolyte interface.

Results

Figure 1a shows the cyclic voltammetry of Si(100), 100nm SiO_2/Si(100) and 300nm SiO_2/Si(100) electrodes using 1.2 M $LiPF_6$/EC:DEC (3:7 wt%) electrolyte. The result shows that Si (100) exhibit different electrochemical behavior as the thickness of the oxide layer varies. The cathodic current around 1 V increases and becomes broader as the oxide thickness increases which could be attributed to either the irreversible reduction of the oxide or the oxide layer modifies the electrolyte reduction mechanism and increased the interfacial reactivity. In the reverse scan, higher reversible capacity was observed for Si(100) with native oxide

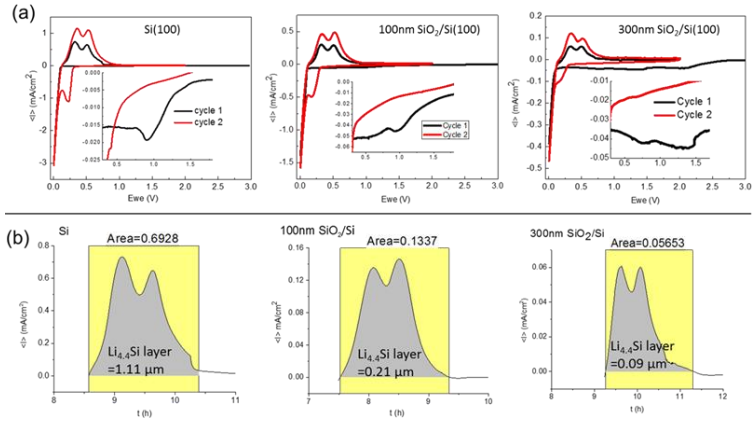

Figure 1. (a) Cyclic voltammetry (b) thickness of hypothetical Li4.4Si layer of Si(100) wafer, 100nm SiO_2/Si(100) and 300nm SiO_2/Si(100) swept from OCV to 0.005V and back to 2 V in 1.2 M LiPF6/EC:DEC (3:7 wt%) electrolyte

layer and the reversible capacity decreases as the oxide thickness increases. Figure 1b shows the thickness of hypothetical Li4.4Si layer assuming the complete lithiation of Si(100) electrode based on equation 1. The result reveals that the thickness of the hypothetical Li4.4Si layer deceases by an order of magnitude as the thickness of the oxide layer increases suggesting that the thermal oxide acts as a barrier for bulk lithiation.

$$Si + 4.4Li^{+} + 4.4e^{-} \rightarrow Li_{4.4}Si \qquad (1)$$

Ex-situ SEM morphology and cross-sectional images of Si(100), 100nm SiO_2/Si(100) and 300nm SiO_2/Si(100) electrodes after 2nd cycle are shown in Figure 2. The samples in these images were extensively rinsed in dimethyl carbonate to remove any residual electrolyte or soluble electrolyte reaction products. Surface cracking due to the lithium insertion and extraction process is clearly observed on the Si(100) electrode (Figure 2a). However, surface of the 100nm SiO_2/Si(100) and 300nm SiO_2/Si(100) electrodes remains smooth after 2 cycles. To investigate if the Si underneath the SiO_2 layer is cracked, cross-sectional SEM analysis has been performed (Figure 2b). The Si(100) cross-section evidently shows the cracking of Si surface and a thickness of ~1.5 µm Si surface delamination. The thickness of the delaminated surface is close to the thickness of hypothetical $Li_{4.4}Si$ layer (1.1µm) calculated from the CV. The cross-section of the thermal oxide samples shows that the Si underneath is not cracked indicating that the amount of lithium inserted and extracted is not enough to cause the cracking of the Si electrode surface underneath the thick oxide layer. This is consistent with the observed lessening of lithium transport through the oxide layer and the formation of thinner $Li_{4.4}Si$.

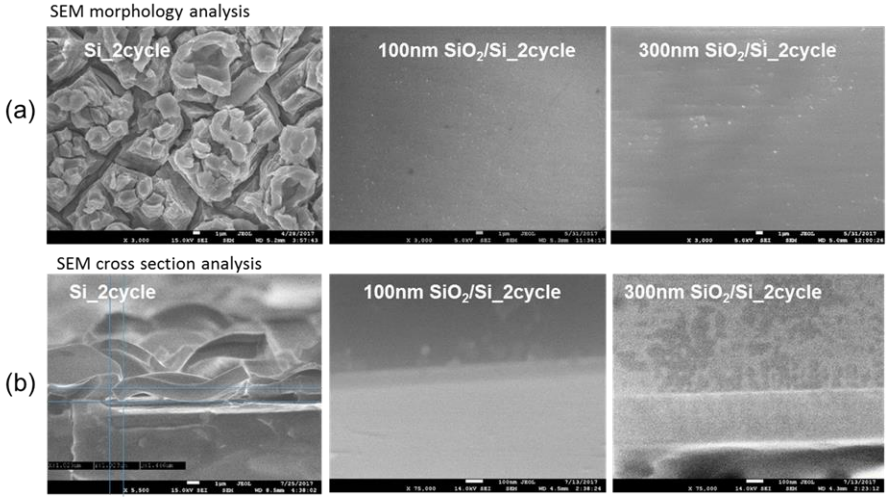

Figure 1. (a) Scanning electron microscopy (SEM) morphology image (b) SEM cross section image of Si(100) wafer, 100nm SiO2/Si(100) and 300nm SiO2/Si(100) after 2 cycles

Conclusions

The electrochemical properties of Si wafers with thermally grown oxides were studied accompanied by post-mortem analysis of the surface chemistry. The results indicated that the oxide layer in Si anodes can present a barrier for bulk lithiation and prevent the complete lithiation of the underlying Si resulting in decreased reversible capacity. In the present work, the oxide thickness was larger than even the size of the Si particles in current Si anode materials. Hence, thinner oxides (5-20 nm) should be considered for understanding of the effect of the oxide on the interfacial properties of Si anodes. For this purpose, the 100nm SiO_2/Si(100) wafers were shipped to NREL for surface treatment to produce thinner SiO_2 coatings for further studies. In parallel, we are using the various spectroscopic techniques we employ at LBNL to determine the role of the oxide layer using other model systems such as the amorphous Si thin films on Cu from ORNL.

References

[1] B. J. Saint, M. Morcrette, D. Larcher, L Laffont, S. Beattie, J. P. Pérès, D. Talaga, M. Couzi, and J. M. Tarascon, *Adv. Funct. Mater.* **17**, 1765–1774 (2007)

[2] K. W. Schroder, A. G. Dylla, S. J. Harris, L. J. Webb, and K. J. Stevenson, *ACS Appl. Mater. Interfaces*, **6** (23), 21510–21524 (2014)

[3] B. Philippe, R. Dedryèvre, J. Allouche, F. Lindgren, M. Gorgoi, H. Rensmo, D. Gonbeau, and Kristina Edström, *Chem. Mater.*, **24**, 1107−1115 (2012)

SEI Characterization – Fluorescent Probes (NREL)

Wade Braunecker - NREL

Background

A variety of methods have been employed to characterize the properties of lithium ions as they are relevant to battery technology, but typically these techniques either require highly specialized equipment (neutron scattering, neutron tomography), do not have the spatial resolution to probe micro- and nanostructured ion transport pathways (NMR), or do not probe the lithium ions themselves but rather assumed ion transport tunnels (scanning probe microscopy, X-ray tomography). Very recently, fluorescence microscopy was proposed as a tool that could potentially satisfy all of these technical obstacles by providing high spatial and time resolution information about the distribution of lithium ions using relatively accessible equipment.[1] However, many technical obstacles remain before such a technique could be employed *in operando* to assess structural information in lithium ion batteries.

Here, we aim to develop fluorescent probes that will help determine how components of the silicon SEI layer evolve with cycling. The work specifically contributes to the SEISta project milestones by complimenting existing strategies to quantitatively measure soluble components of the SEI as well as measure the growth rate of the SEI components at fixed potentials and during cycling.

Results

This quarter, work commenced with the synthesis of a model fluorescent probe recently described in the literature (Figure 1) that is highly sensitive and specific to lithium ions.[1] The organic molecule 2-(2-hydroxyphenyl)-naphthoxazole (HPNO) reportedly binds lithium in a 2:1 stoichiometry and maintains tetrahedral geometry, but the binding planarizes the organic molecule, which in turn red shifts its absorbance and fluorescence spectra. Following the synthesis and characterization of HPNO this quarter, we verified the response of its optical properties to increasing lithium ion concentration with simple solution absorbance measurements. As can be seen in Figure 1, absorbance red-shifts more than 40 nm in the presence of LiBr, and absorbance intensity scales with LiBr concentration.

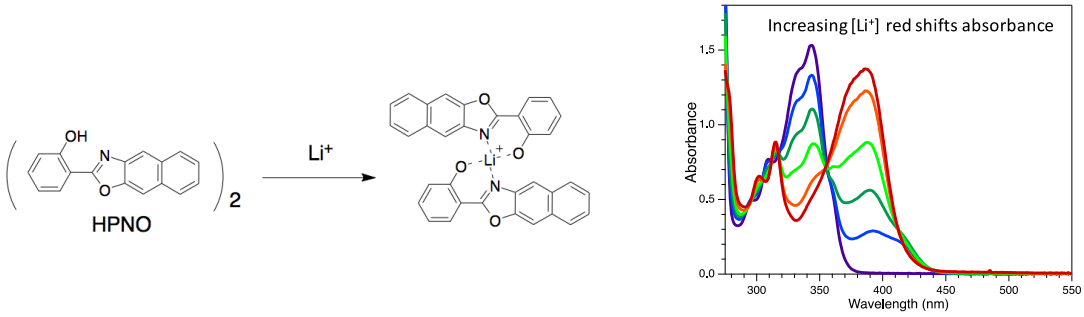

Figure 1. (Left) Scheme for lithium binding by HPNO fluorophore. (b) UV-vis spectra of 0.05 mM HPNO in propylene carbonate without lithium (purple) and increasing amounts of LiBr until the solution is saturated with LiBr (red).

We then designed and implemented a three-step synthetic route to covalently tether this fluorescent probe into 2 different model binder systems commonly employed with silicon anode materials. These polymeric binders are currently being characterized, after which absorbance spectra and fluorescence quenching dynamics will be studied as a function of the chemical composition of the binder, fluorescent probe density, gel-crosslinking density, concentration of conductive additives in the gel, etc., in order to establish a fundamental picture of how these probes might behave *in operando*.

Conclusions

Initial work this quarter has verified that a fluorescent probe recently developed in the literature does indeed show an excellent optical response to the presence of lithium ions in solution. A novel synthetic pathway for covalently incorporating this molecule into two different polymer binders commonly employed with silicon anodes was developed and implemented. Full characterization of the materials is underway.

References

1. N. A. Padilla, M. T. Rea, M.Foy, S. P. Upadhyay, K. A. Desrochers, T. Derus, K. A. Knapper, N. H. Hunter, S. Wood, D. A. Hinton, A. C. Cavell, A. G. Masias, R. H. Goldsmith, "Tracking Lithium Ions via Widefield Fluorescence Microscopy for Battery Diagnostics", *ACS Sens.* **2017**, *2*, 903-908.

SEI Characterization - Tip Enhanced Raman Spectroscopy (TERS) (ORNL)

Guang Yang (ORNL) and Jagjit Nanda (ORNL)

Background

In the last quarter we reported the TERS maps for 1x, 5x and 20x cycled amorphous Si fabricated at ORNL. The spectral imaging showed evidence of compositional changes of SEI as we progressively cycled the silicon (from 1x to 20x). We further analyzed the chemical signature of the SEI film from the TERS signal. This quarter we correlated the topography of SEI layer with the chemical compositional (TERS) maps to highlight the various SEI phases that are Raman active. TERS by nature is only sensitive to top 50 nm of SEI surface and thereby can monitor the changes in the surface chemical composition as Si is cycled. These results will be compared with results with XPS and ToF-SIMS as dimmed necessary (in collaboration with other SEIsta PI's)

Results

Amorphous silicon was sputtered on the copper electron collector at ORNL and cycled as per the procedure finalized by the round robin team of SEIsta. The silicon is 20 nm thick measured by the quartz crystal microbalance. The amorphous silicon samples were further cycled 1x, 5x and 20x times using 1M $LiPF_6$ in EC/DEC (1:1 vol). TERS experiments were performed using a HORIBA Xplora Nano Raman Platform integrated with AIST-NT SPM system. The laser wavelength was 532 nm and the objective was 100x/0.7 N.A.. The laser power was set at 100 µW. The TERS tip was fabricated by thermal evaporating 2 nm chromium on commercial Bruker silicon tip (26 N/m, 300 kHz), followed by coating a 40 nm silver layer. Another layer of aluminum was coated on top as a protection layer. All TERS measurements were performed in a special Ar-compatible antechamber to avoid air exposure.

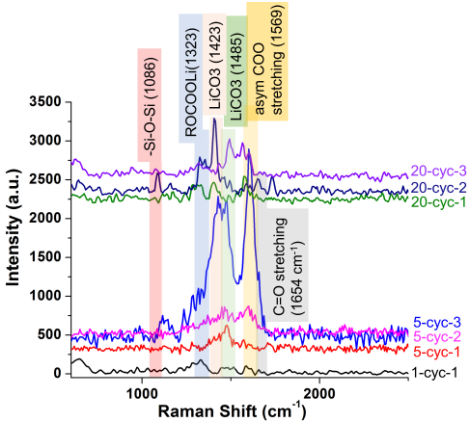

Figure 3 TERS spectra taken from different samples on various locations on cycled amorphous Si (ORNL)

The TERS laser power was about 100 µW, which avoids possible decomposition of SEI by laser-induced heating. It is noteworthy that as such low laser power normal micro-Raman cannot detect any signal from the SEI. However, distinguished TERS bands were observed for amorphous silicon samples of different cycle numbers (Figure 1). To get an idea of the spatial inhomogeneity of the SEI, we report 3 TERS spectrum collected at different sample locations as shown in Fig.1. For the 1x-cycled sample, a band centered at around 1323 cm^{-1} was observed, attributed to ROCOOLi species. This could be primarily from the EC decomposition during the first cycle. The band between 1000 and 1100 cm^{-1} is assigned to siloxane (Si-O-Si). For the 5x-cycled sample, we notice relatively high TERS intensity from the asymmetric -COO stretching at 1569 cm^{-1} and also the $LiCO_3$ peak at 1423 cm^{-1} and 1485 cm^{-1} at specific locations (e.g. location 3 in Figure 2). For the 20x-cycled sample, we see a relatively strong carbonate signal, with lower ROCOOLi component. We notice that the TERS spectra are spatially inhomogeneous for each cycled sample. TERS mapping would be a good way to look at such spatial variation as shown below.

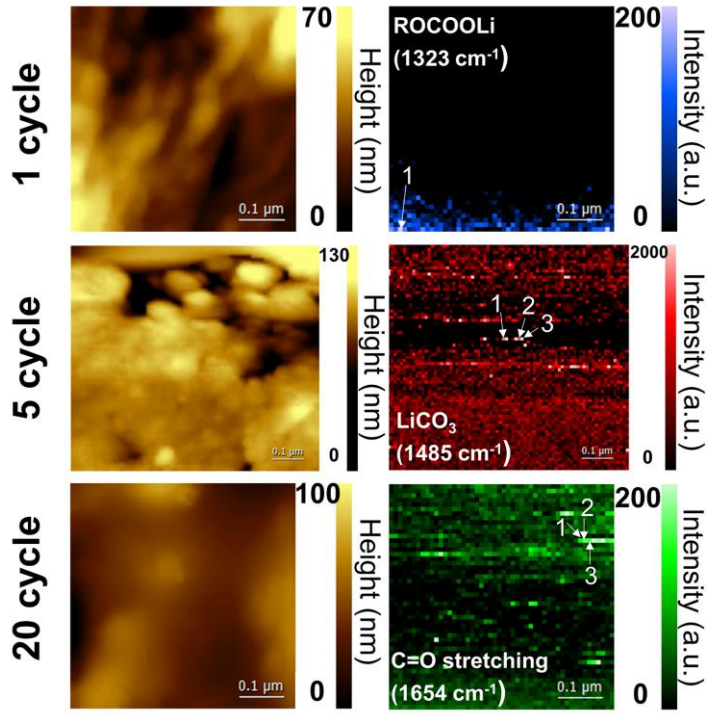

Figure 2. AFM topography and the corresponding TERS map for each Si/Cu sample showing the heterogeneous distribution of the SEI. The number label on the TERS map corresponds to that for TERS spectra taken at different locations of each sample in Figure 1. The scanning size is 500x500 nm^2 for 1-cycle and 20-cycle samples, and 700x750 nm^2 for 5-cycle samples.

Figure 2 shows the topography and the corresponding chemical spectrum at the same spatial location. The TERS map was generated by the characteristic peak integration for each band with the scanning step size set at 10 nm. The TERS map for 1-cycle silicon indicates that the ROCOOLi component preferably distributes at the lower part of the scanned area. For the 5x-cycle sample, $LiCO_3$ distribution was mapped by integrating 1485 band. The spectral difference between locations 2 and 3 (also see Figure 1) clearly indicates that TERS is capable of characterizing nanoscale spatial heterogeneity of the SEI (the distance between Location 2 and 3 is 10 nm). Similar observation was made for 20x-cycle silicon. The consequent three locations with 10 nm distance between each exhibit different spectral intensities and features (labeled as 20x-cyc-1, 20x-cyc-2 and 20x-cyc-3 in Figure 1). One example shown in 20x-cycled sample is the distribution of the C=O stretching band at 1654 cm^{-1}.

Conclusions

The data show the chemical heterogeneity of the SEI layer. This method will now be applied to SEISta electrodes on copper foil or after cycling at LBNL.

SEI Characterization - Analytical Microscopy (NREL)

Caleb Stetson, Seoung-Bum Son, Andrew Norman, Chun-sheng Jiang, Mowafak Al-Jassim (NREL)

Background

Instability of the organic electrolyte at lower voltage results in the decomposition of electrolyte and formation of the solid electrolyte interface (SEI) on the surface of anode materials. The SEI is generally composed of organic/inorganic species and known for electronic insulation that disturbs further electro-chemical reaction in the battery. Our group has adapted scanning-spreading resistance microscopy (SSRM) to measure the local electronic resistivity of SEI with high lateral and vertical spatial resolution. We found that the electronic resistivity decreases sharply from the SEI surface toward the Si anode and the decrease depends on the formation conditions of the SEI, such as electrochemical cycling. In this quarter for the validation and calibration of SSRM, we have measured an amorphous Si (α-Si) layer-stack sample with well-controlled resistivities and thicknesses. We have also measured the resistivity profile of SEI formed with different electrolytes. To better understand the importance of SEI structure and composition to battery performance, it is critical to determine the chemical composition and thicknesses of SEI layers formed on Si electrodes after cycling. We report STEM imaging and EELS and EDS analysis of the SEI layer formed on a Si wafer round robin sample with a native oxide layer after 2 cycles in Gen2 electrolyte. (1.2 M $LiPF_6$ in ethylene carbonate: ethylmethyl carbonate (3:7 by weight)).

Electronic resistance versus SEI stability: Electronic resistance of SEI is believed to be a critical property in the larger goal of stabilizing the SEI on Si. An SEI with low electronic resistance will encourage further electrolyte decomposition and SEI growth, resulting in lower coulombic efficiencies and shorter battery lifetime. More resistive SEI electronically passivates the anode, limiting electrolyte decomposition and SEI growth and thus improving the battery lifetime. While impedance spectroscopy provides useful information regarding the resistance properties of the overall system, our group's novel instrumental approach provides unparalleled nanoscale resolution in the lateral and vertical directions under the various electrolytes circumstances.

Electronic resistance sensitivity to chemical composition: The measured local spreading resistance is determined by the chemical composition and structures of the SEI. Resistance vs. depth profiles of SEI on Si demonstrate high resistance in the near-surface region of the SEI, indicating an organic-rich composition, while the relatively lower resistance in the near-Si region is indicative of an inorganic-rich composition. This behavior also varies by additions of FEC and various Li salts, which gives an idea of ideal electrolyte additives to form stable SEI on the surface. Pairing high spatial resolution SSRM data for SEI with chemical characterization data provides a more complete picture of the SEI compositional segregation. Thus far, analysis of SEI on Si has revealed high levels of lateral homogeneity but significant chemical segregation moving from the surface of the SEI to the interface with the Si anode material. This technique has the added utility of recognizing any potential lateral inhomogeneity in SEI composition, as it is sensitive to differences in local electronic resistance.

SEI thickness measurement: The conductive properties of Si allow for easy detection of the Si/SEI interface, allowing for accurate and rapid measurement of total SEI thickness.

SEI surface morphology: Lastly, AFM-based morphology studies of SEI (taking into account the original anode morphology) provide important information regarding SEI formation and evolution.

Results

For the reference sample, three distinct layers of Phosphorous-doped α-Si were deposited by PECVD (Bill Nemeth at NREL Si group), on an N-type Si wafer, where thicknesses and resistivities of each layer were measured by depositing "sister" films.

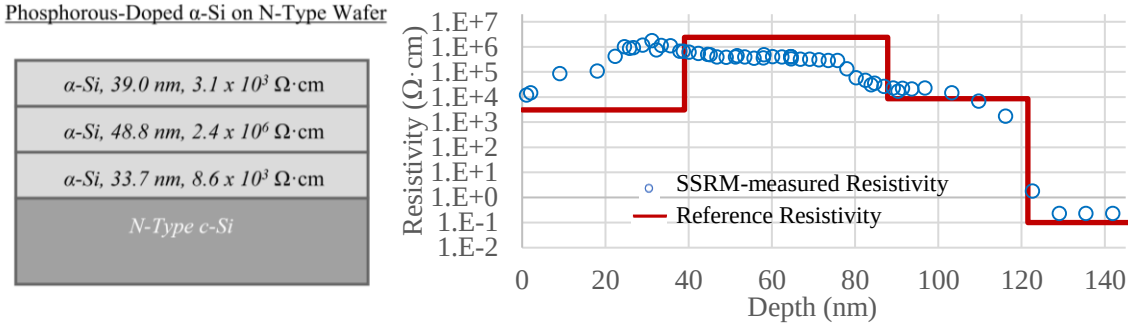

Figure 1. Si Reference Sample Schematic and Results of SSRM Depth Profiling.

The results of SSRM resistance profiling is semi-quantitatively consistent with the designed resistivities (Figure 1). The differences between the reference resistivities and SSRM-measured resistivities can be due to multiple factors: instrumental resolution (i.e. the radius of the spreading resistance), non-ideality of doping in the prepared Si reference sample, and inter-diffusion of the dopant between the layers during the high-temperature deposition.

In addition to validating our instrumentational technique with the prepared Si reference sample, investigation of SEI with SSRM depth profiles has continued. Characterization of Si wafers cycled with different electrolytes (prepared by Taeho Yoon and Chunmei Ban) shows consistent results of a sharp resistance decrease from the SEI surface toward the Si. However, the electrolytes have significant effects on the overall resistance value and SEI thickness. Both the resistance values and thicknesses of SEIs formed from varied electrolytes exhibit the trend (inorganic salt + FEC) > (organic salt) > (inorganic salt), indicating that the electrolyte plays an important role in the formation and characteristics of the SEI (Figure 2). In the last quarter, our group has also performed morphological studies of Si anode materials and SEI with atomic force microscopy (AFM).

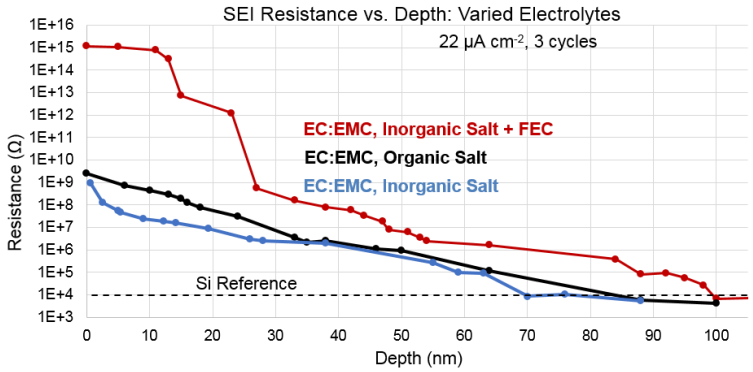

Figure 2. SSRM Resistance vs. Depth Profiles of SEIs on Si Wafers Cycled with Varied Electrolytes.

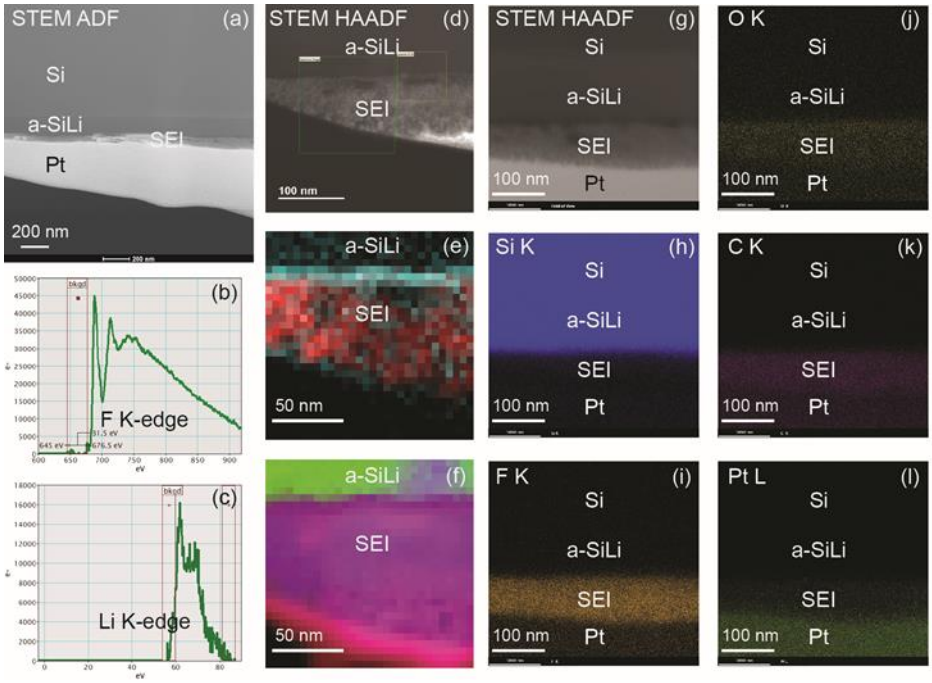

Figure 3. STEM imaging, EELS, and EDS analysis of SEI layer formed on a Si wafer round robin sample with native oxide layer after 2 cycles in Gen2 electrolyte. (a) STEM ADF image showing irregular thickness SEI layer and ~ 200 nm thick amorphous SiLi alloy layer formed after 2 cycles. (b) and (c) EELS spectra from SEI layer showing clear F K and Li K edges. (e) RGB STEM EELS areal density map of F (red) and O (cyan); and (f) C (red), Si (green), and Li (blue) distributions. (g) to (l) STEM HAADF image and EDS atomic % maps of Si, F, O, C, and Pt.

Figure 3 shows the STEM imaging and analysis performed by FIB. The results revealed that the major elements in an SEI appear to be Li and F, which is consistent with the literature reporting LiF as a main SEI component in the carbonate based electrolyte. C and O are also present in the SEI layer but little P was detected by either EELS or EDS.

Conclusions

Characterization of a known Si reference sample demonstrated that SSRM is capable of measuring the local electronic resistance via depth profiling. We have continued SSRM electronic resistance depth profiling on SEI, and found significant effects of electrolyte on SEI resistance and thickness. STEM characterization of a cycled Si wafer indicated that the major component of the SEI layer in the sample examined is LiF.

This work was supported by the U.S. Department of Energy under Contract No. DE-AC36-08GO28308 with Alliance for Sustainable Energy, LLC, the Manager and Operator of the National Renewable Energy Laboratory. Funding provided by U.S. Department of Energy Office of Energy Efficiency and Renewable Energy Vehicles Technologies Office.